SPECIAL ISSUE

TECHNICAL, SCIENTIFIC
AND
RESEARCH REPORTS

VOL.10 (2018)

Typical atmospheric scenarios in the 0.6 - 5 THz wavelength range

(REPORT - DIAST Project)

TSRR

IFAC-TSRR vol. 10 (2018) 49-96

Typical atmospheric scenarios in the 0.6-5 THz wavelength range

(REPORT - DIAST Project)

Vanni Nardino[1,*], Massimo Baldi[1,**]

([1]) "Nello Carrara" Institute of Applied Physics, CNR Florence Research Area, Via Madonna del Piano 10, 50019 Sesto Fiorentino (FI), Italy

([*]) v.nardino@ifac.cnr.it
([**]) m.baldi@ifac.cnr.it

 ISSN 2035-5831

Contents

1 Introduction

1.1 THz frequency range

This report presents an analysis of the atmospheric characteristics in the terahertz spectral region (frequencies from 300 GHz to 10 THz, wavelengths from 30 μm to 1 mm, see Fig. 1.1), with particular attention in the range 1 to 5 THz. This interval is the spectral range of interest in the framework of DIAST project.

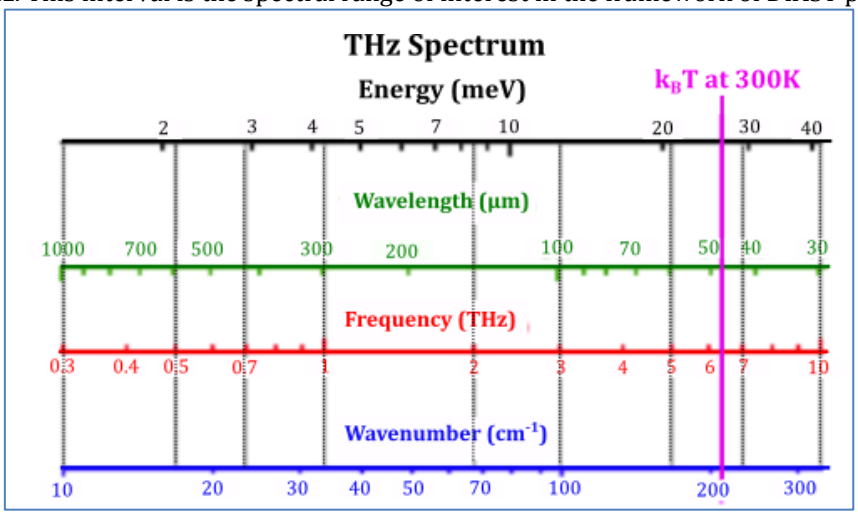

Fig. 1.1: Different scales and units.

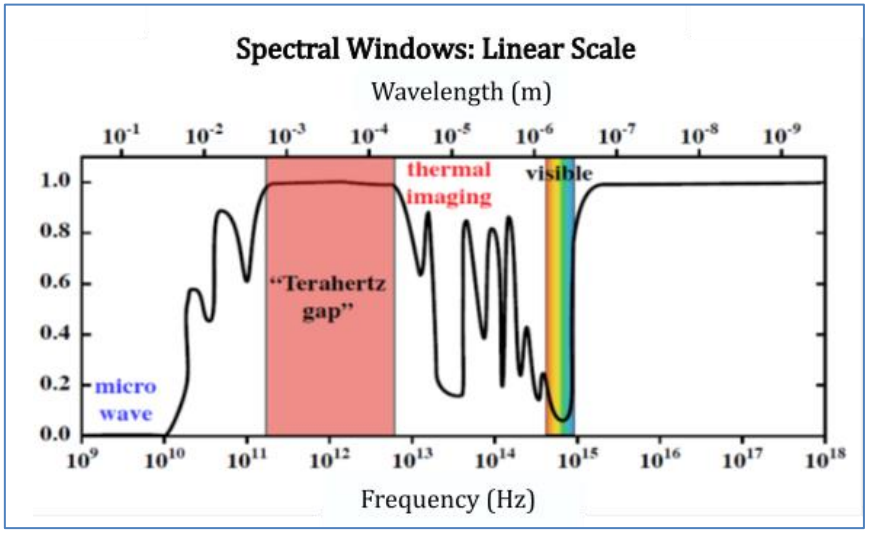

Fig. 1.2: Absorption spectral windows.

Historically the THz spectral interval has been characterized by a relative lack of convenient radiation sources, detectors and transmission technology (Fig. 1.2).

The simulated atmospheres presented in this document will be considered during the designs of different spectroradiometers and for the simulation of their instrumental responses.

The atmospheres have been chosen to be representative of a realistic working scenario in different acquisition geometries, taking into account the typical gaseous components and pollutants of terrestrial atmosphere.

2 Atmospheric scenario in the range 600 GHz – 5 THz

2.1 *Mathematical background*

In a homogeneous medium (i.e. a layer in a constant, stratified atmosphere), the monochromatic radiance I (i.e. power for normal area, solid angle units) extincted in an infinitesimal layer ds is:

$$dI = I(s + ds) - I(s) = -\beta_e(s)I(s)ds$$

being β_e the extinction (scattering plus absorption) coefficient.

Neglecting the scattering ($\beta_e = \beta_a$, being β_a the absorption coefficient) we can express the infinitesimal absorbed radiance dI_{abs} as:

$$dI_{abs} = -\beta_a I ds$$

On the other hand, the emitted radiance dI_{emit} is (Kirchhoff's Law):

$$dI_{emit} = \beta_a B(T) ds$$

being $B(T)$ the blackbody radiance (Plank's Law) as a function of temperature T:

- $B(T) = \frac{2hf^3}{c^2}\frac{1}{e^{\frac{hf}{kT}}-1}$, for the frequency f;
- $B(T) = \frac{2hc^2}{\lambda^5}\frac{1}{e^{\frac{hc}{\lambda kT}}-1}$, for the wavelength λ;
- $B(T) = 2hc^2\nu^3\frac{1}{e^{\frac{hc\nu}{kT}}-1}$, for the wavenumber $\nu = \frac{1}{\lambda}$;

with k being the Boltzmann constant and h the Plank constant.

The radiance balance is therefore:

$$dI = dI_{abs} + dI_{emit} = \beta_a(B(T) - I)ds$$

Defining the optical depth as $\tau = \beta_a s$, the equation above can be integrated along an optical depth τ, bringing to:

$$I(0) = I(\tau)e^{-\tau} - B(T)(e^{-\tau} - 1)$$

where $I(0)$ is the received radiance and $I(\tau)$ a source term at distance $s = \frac{\tau}{\beta_a}$.

The HITRAN interface neglects any source term for simulating the radiance emitted by an homogeneous medium. The simulations shown in next paragraph are obtained by the formula:

$$I = B(T)(1 - T(p,T))$$

being $T(p,T) = e^{-\tau} = e^{-s\beta_a(p,T)}$ the transmittance depending (through β_a) by the medium temperature and pressure for taking into account the absorption/emission line shaping effects.

Being the HITRAN a spectral line database, for simulating the emission of a generic custom atmosphere, the HITRAN interface used (HITRAN On The Web applet at hitran.iao.ru/home) calculates the absorption coefficient for a user-selected gas mixture using the following formulas.

Being $K_{a_{jm}}$ the monochromatic absorption line coefficient for a single molecular species for volume unit, for a single spectral line corresponding to a transition between levels j and m at a given pressure p and temperature T, The absorption coefficient K_a at wavenumber WN (in cm^{-1}), for a single molecule per unit volume is obtained by summing over all the transitions $j \rightarrow m$:

$$K_a(WN,T,p) = \sum_{jm} K_{a_{jm}}(WN,T,p) \quad \left[\frac{cm^2}{molecule}\right]$$

For a gas mixture the partial absorption coefficients are weighted with the mixing ratios of these species.

The absorption coefficient β_a $[cm^{-1}]$ is then calculated as:

$$\beta_a(WN,T,p) = N\, K_a(WN,T,p)$$

being N $\left[\frac{molecule}{cm^3}\right]$ the number of absorbing molecules per volume unit considering a perfect gas.

2.2 *Pollutant signal in atmospheric radiance: constant path*

For this analysis, we have chosen the US-Standard 1976 atmosphere as *unpolluted* representative atmosphere. We have set up three scenarios (using the HITRAN On The Web applet), as shown in the following table:

	Press. (Atm)	Press. (hPa)	Temp.(K)	Altitude a.s.l. (km)	N2 (%) (1)	O2 (%)	H2O (ppm)	CO2 (ppm)	O3 (ppm)
low stratosphere	0.1	100	216	16	78.26615	21.70000	5.0	333 (2)	0. 5
mid stratosphere	0.01	10	227	31	78.26560	21.70000	5.0	333 (2)	6.0
high stratosphere	0.001	1	270	48	78.26595	21.70000	5.0 (3)	333 (2)	2.5

(1): N2 concentration is used for normalizing the sum to 100%.
(2): Underestimated with respect to actual values (the reference atmosphere is US 1977) but uninfluential.
(3): for high stratosphere overestimated water value (for worst-case scenario).

For investigating the effects of different pollutants present in the atmosphere and of some interest for remote sensing measurements, we simulated the effects of a pure N2 atmosphere (transparent in the frequency range of interest) with each pollutant in realistic atmospheric concentration. For pollutant present only in traces in atmosphere, we saturated the concentration to the minimum concentration of 1.E-08 (ratio in volume).

The pollutant list is detailed in the following table, together with the concentration used.

Applying the formulas described in par. 2.1, we have simulated the unpolluted atmospheres for each case (Fig. 2.1 - Fig. 2.3), and compared with the ideal corresponding blackbody spectrum.

Using the HITRAN simulation of the polluted atmospheres, the signal due to each single pollutant can be analysed and compared with the background signal, as shown in next paragraphs for each pollutant of the table, compared to the background atmospheric spectrum (Fig. 2.4 - Fig. 2.12).

Pollutant	Atmosphere composition	Concentrations (%)
N2O	N2O 0.28ppm + N2	N_2O: 0.000028 N_2: 99.999972
O3	O3 2 ppm + N2	O_3: 0.000200 N_2: 99.999800
CO	CO 0.47ppm + N2	CO: 0.000047 N_2: 99.999953
CH4	CH4 1.48 ppm + N2	CH_4: 0.000148 N_2: 99.999852
NO	NO 0.01ppm N2	NO: 0.000001 N_2: 99.999999
SO2	SO2 0.08ppm + N2	SO_2: 0.000008 N_2: 99.999992
NO2	NO2 0.01ppm + N2	NO_2: 0.000001 N_2: 99.999999
NH3	NH3 0.01ppm + N2	NH_3: 0.000001 N_2: 99.999999
OH	OH 0.01ppm + N2	OH: 0.000001 N_2: 99.999999
HCl	HCl 0.01ppm + N2	HCl: 0.000001 N_2: 99.999999
H2CO	H2CO 0.01ppm + N2	H_2CO: 0.000001 N_2: 99.999999
HOCl	HOCl 0.01ppm + N2	HOCl: 0.000001 N_2: 99.999999
CH3OH	CH3OH 0.01ppm + N2	N_2: 99.999999 CH_3OH: 0.000001
H2S	H2S 0.01ppm + N2	N_2: 99.999999 H_2S: 0.000001
SO3	SO3 0.01ppm + N2	N_2: 99.999999 SO_3: 0.000001

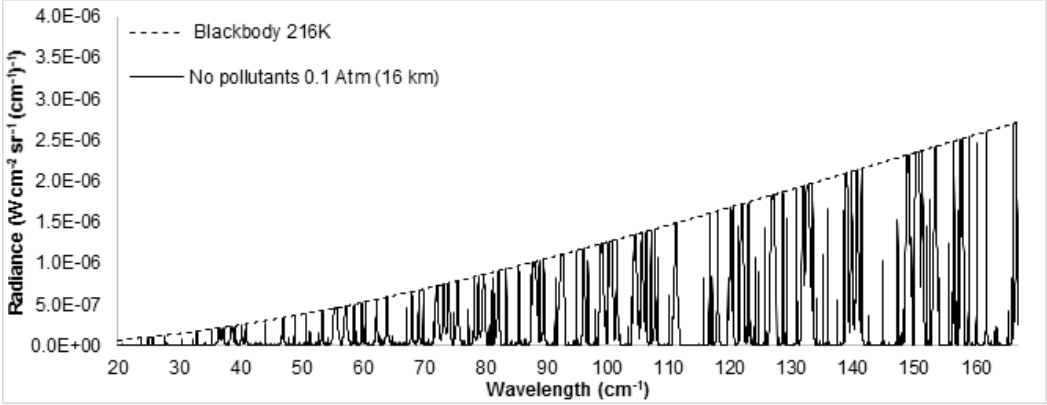

Fig. 2.1: Simulated unpolluted atmospheric path of 10000 m at 0.1 atm. (16 km altitude) and comparison with the corresponding blackbody spectrum.

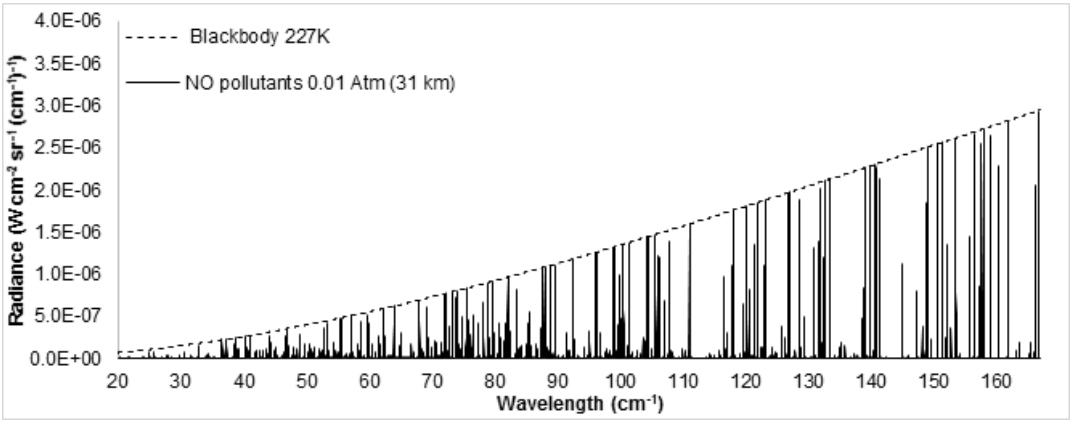

Fig. 2.2: Simulated unpolluted atmospheric path of 10000 m at 0.01 atm. (31 km altitude) and comparison with the corresponding blackbody spectrum.

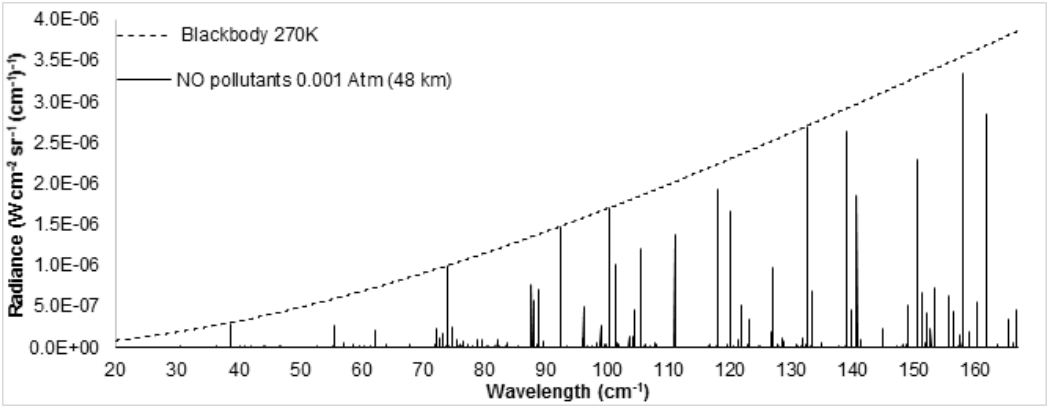

Fig. 2.3: Simulated unpolluted atmospheric path of 10000 m at 0.001 atm. (48 km altitude) and comparison with the corresponding blackbody spectrum.

2.2.1 N2O

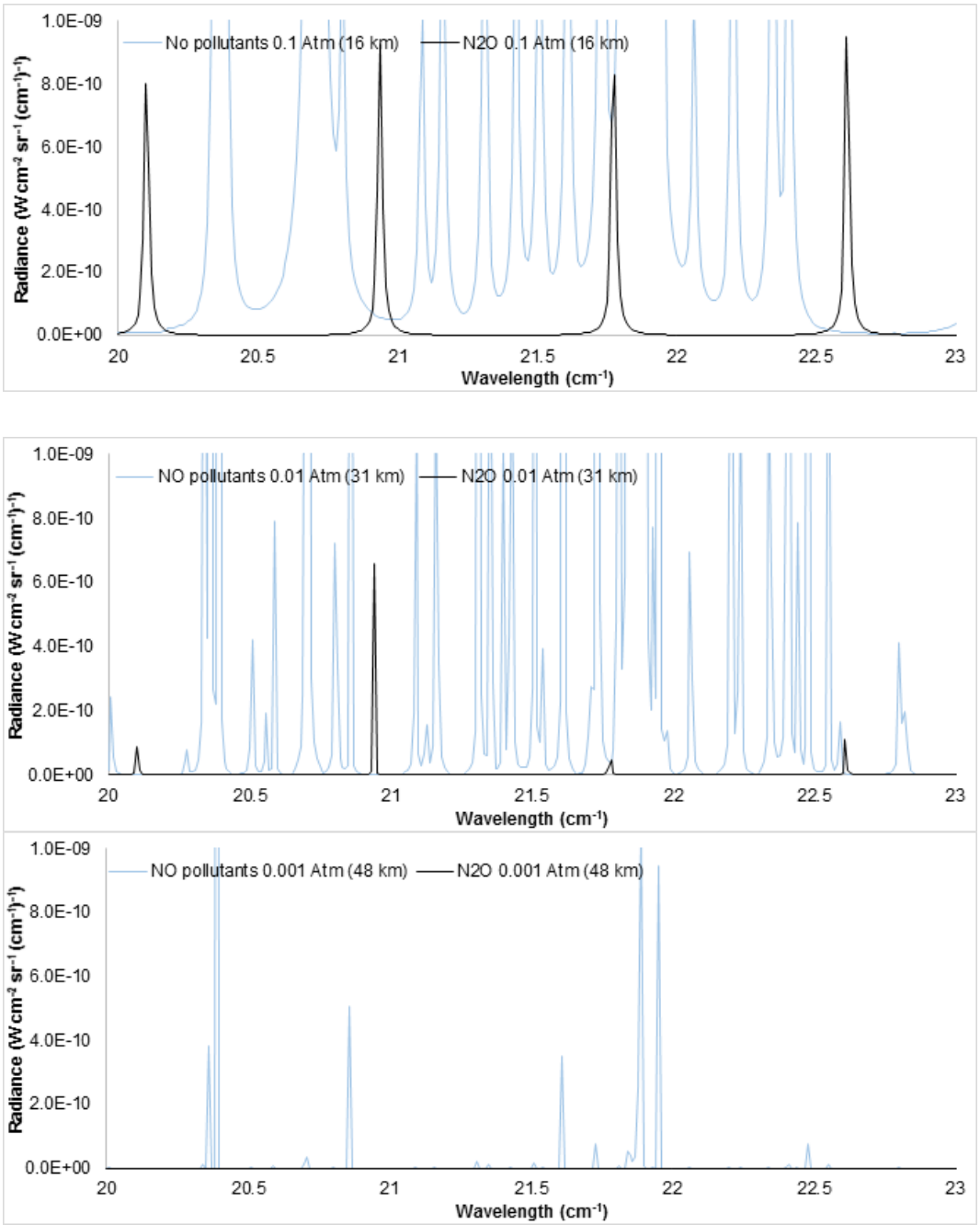

Fig. 2.4: Radiance spectrum with spectral features of the typical concentration of N2O and the spectrum for the corresponding unpolluted atmospheres at 16, 31 and 48 km for a 10000 m homogenous path.

2.2.2 CO

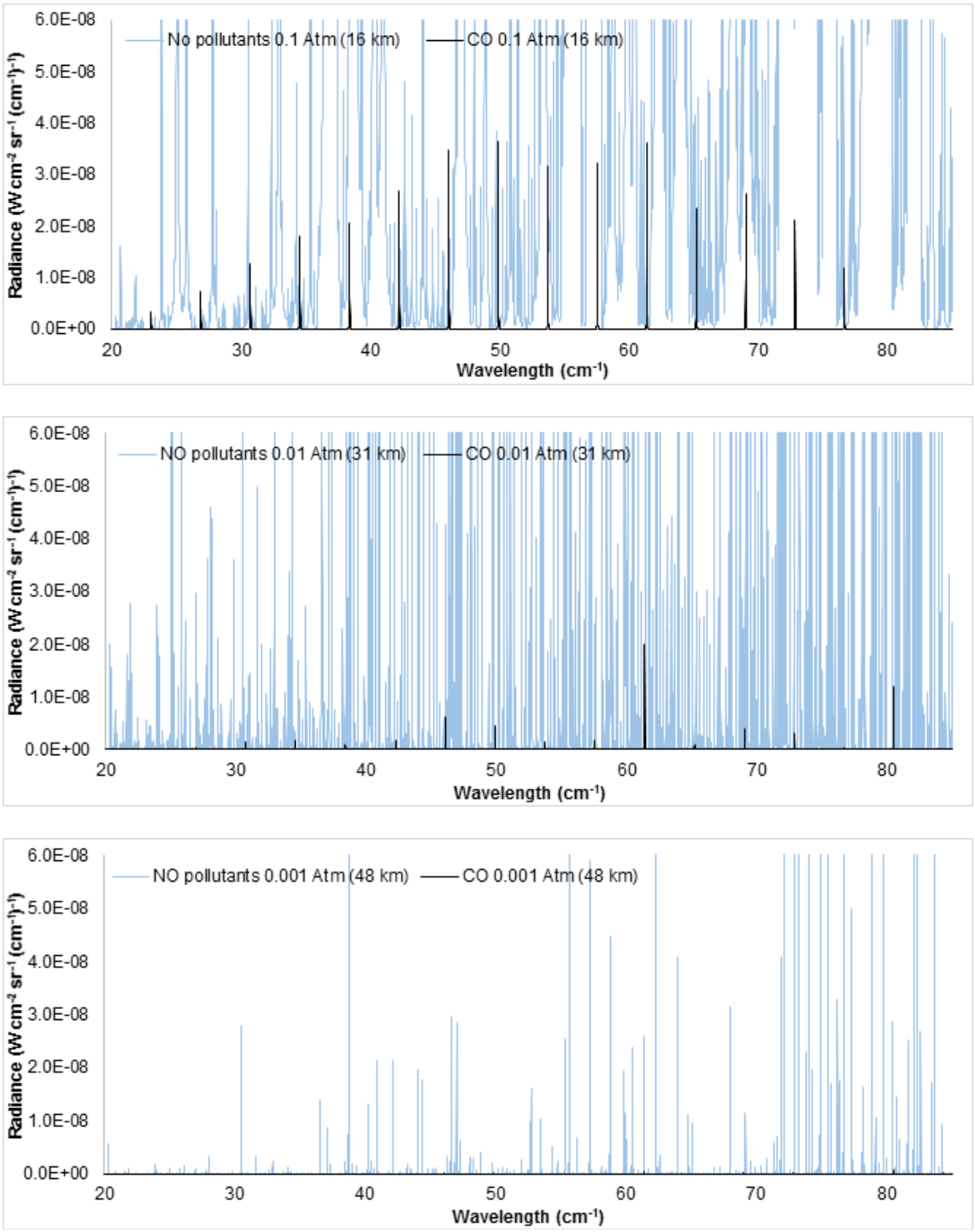

Fig. 2.5: Radiance spectrum with spectral features of the typical concentration of CO and the spectrum for the corresponding unpolluted atmospheres at 16, 31 and 48 km for a 10000 m homogenous path.

2.2.3 SO2

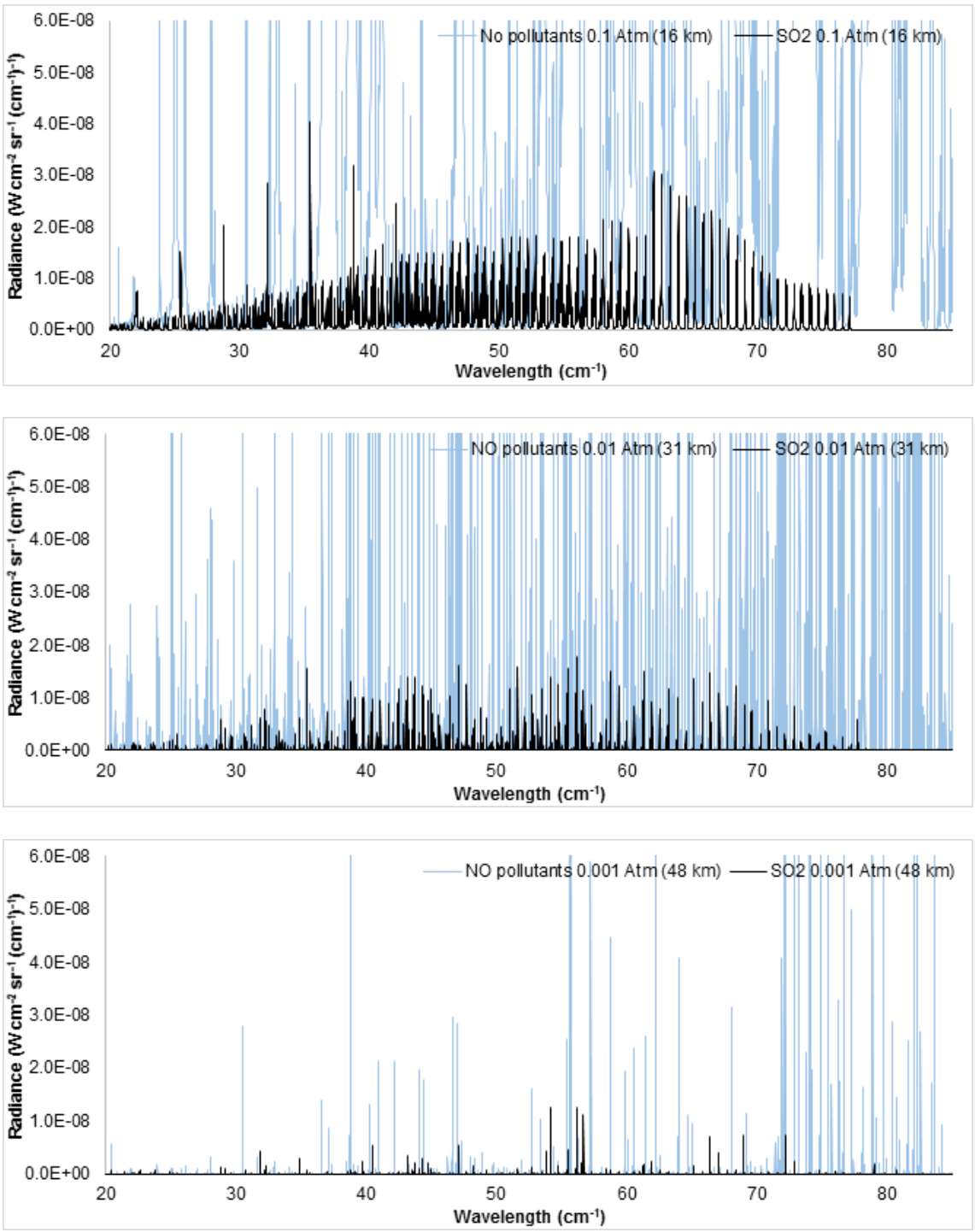

Fig. 2.6: Radiance spectrum with spectral features of the typical concentration of SO2 and the spectrum for the corresponding unpolluted atmospheres at 16, 31 and 48 km for a 10000 m homogenous path.

2.2.4 NH3

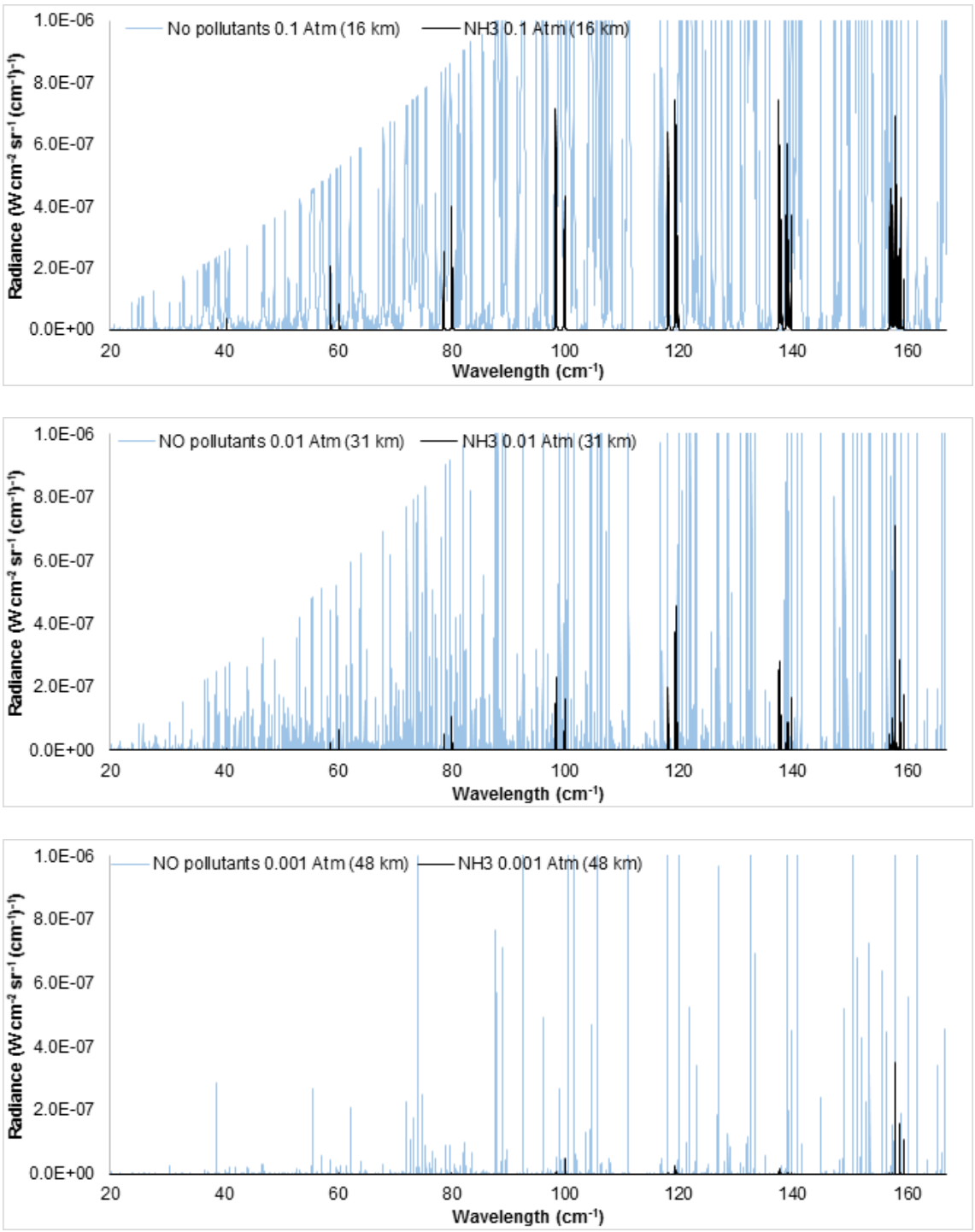

Fig. 2.7: Radiance spectrum with spectral features of the typical concentration of NH3 and the spectrum for the corresponding unpolluted atmospheres at 16, 31 and 48 km for a 10000 m homogenous path.

2.2.5 OH

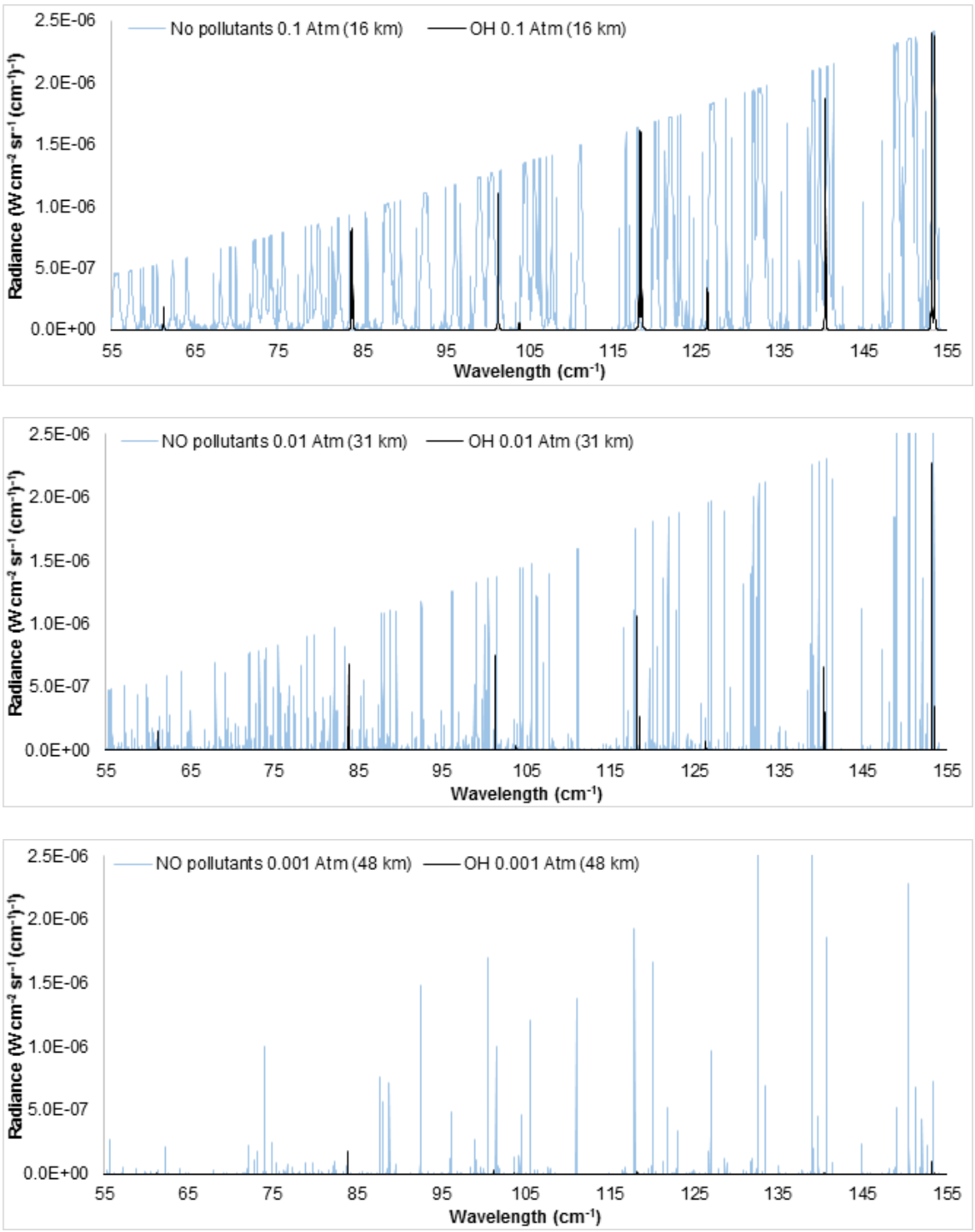

Fig. 2.8: Radiance spectrum with spectral features of the typical concentration of OH and the spectrum for the corresponding unpolluted atmospheres at 16, 31 and 48 km for a 10000 m homogenous path.

2.2.6 HCl

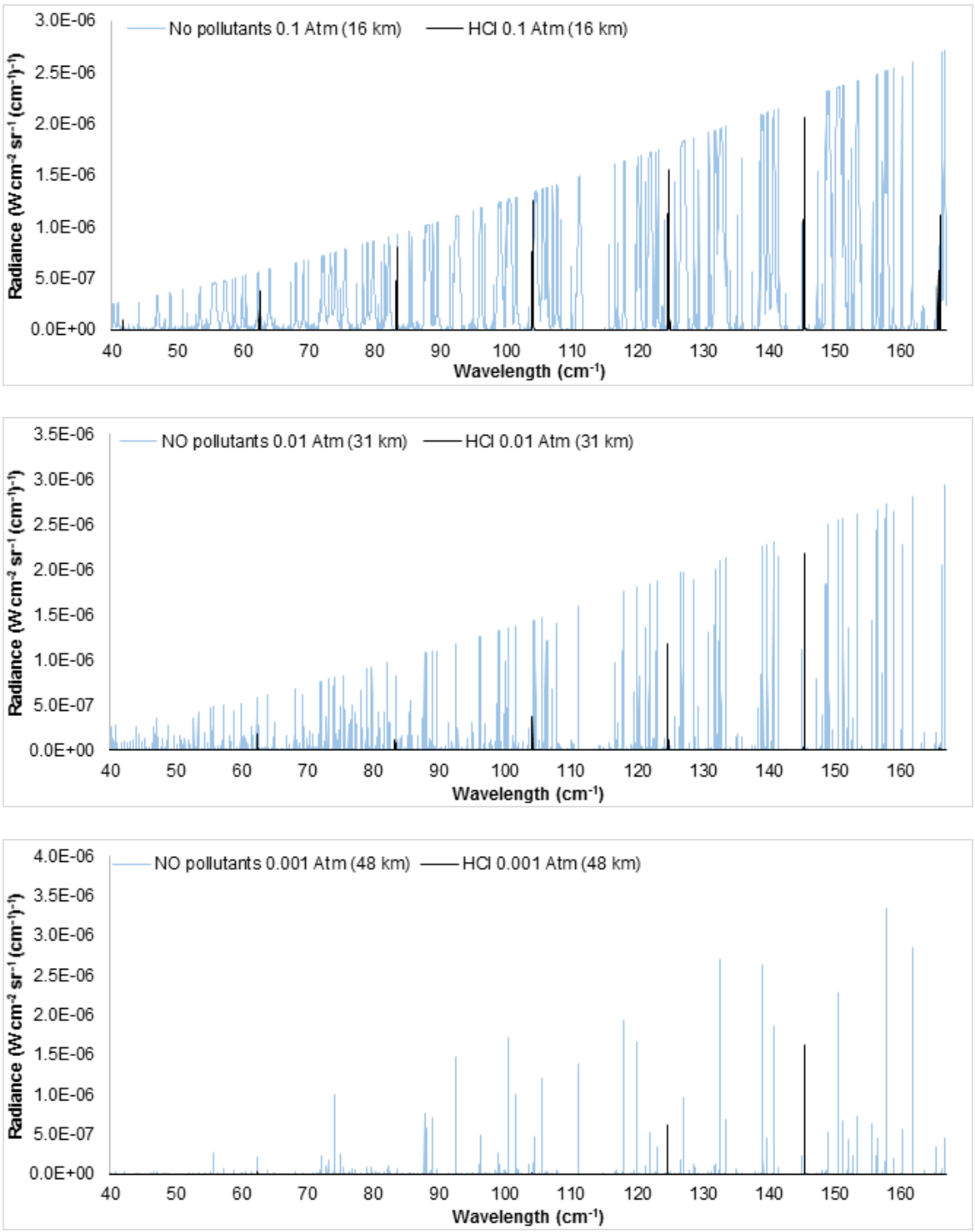

Fig. 2.9: Radiance spectrum with spectral features of the typical concentration of HCl and the spectrum for the corresponding unpolluted atmospheres at 16, 31 and 48 km for a 10000 m homogenous path.

2.2.7 H2CO

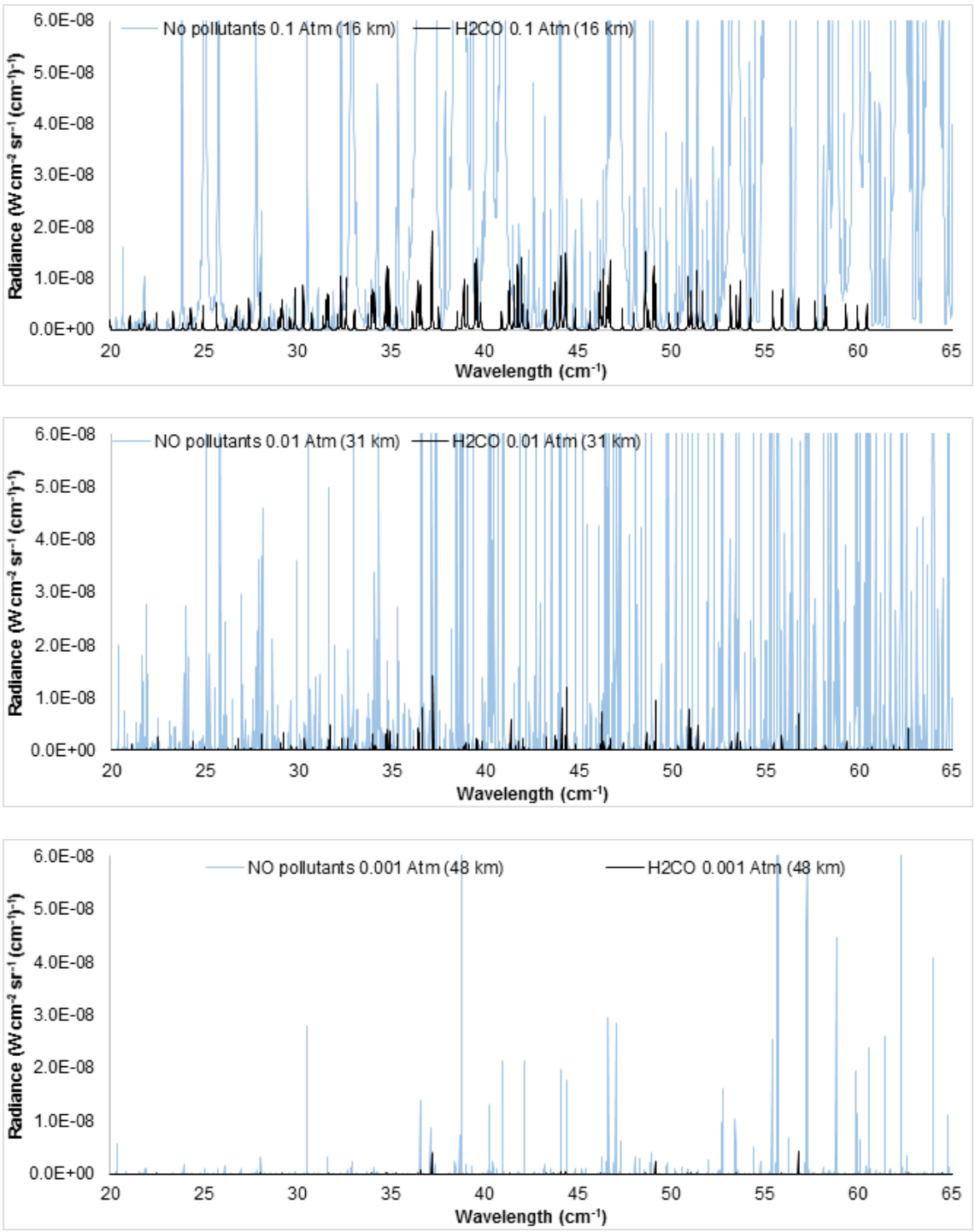

Fig. 2.10: Radiance spectrum with spectral features of the typical concentration of H2CO and the spectrum for the corresponding unpolluted atmospheres at 16, 31 and 48 km for a 10000 m homogenous path.

2.2.8 HOCl

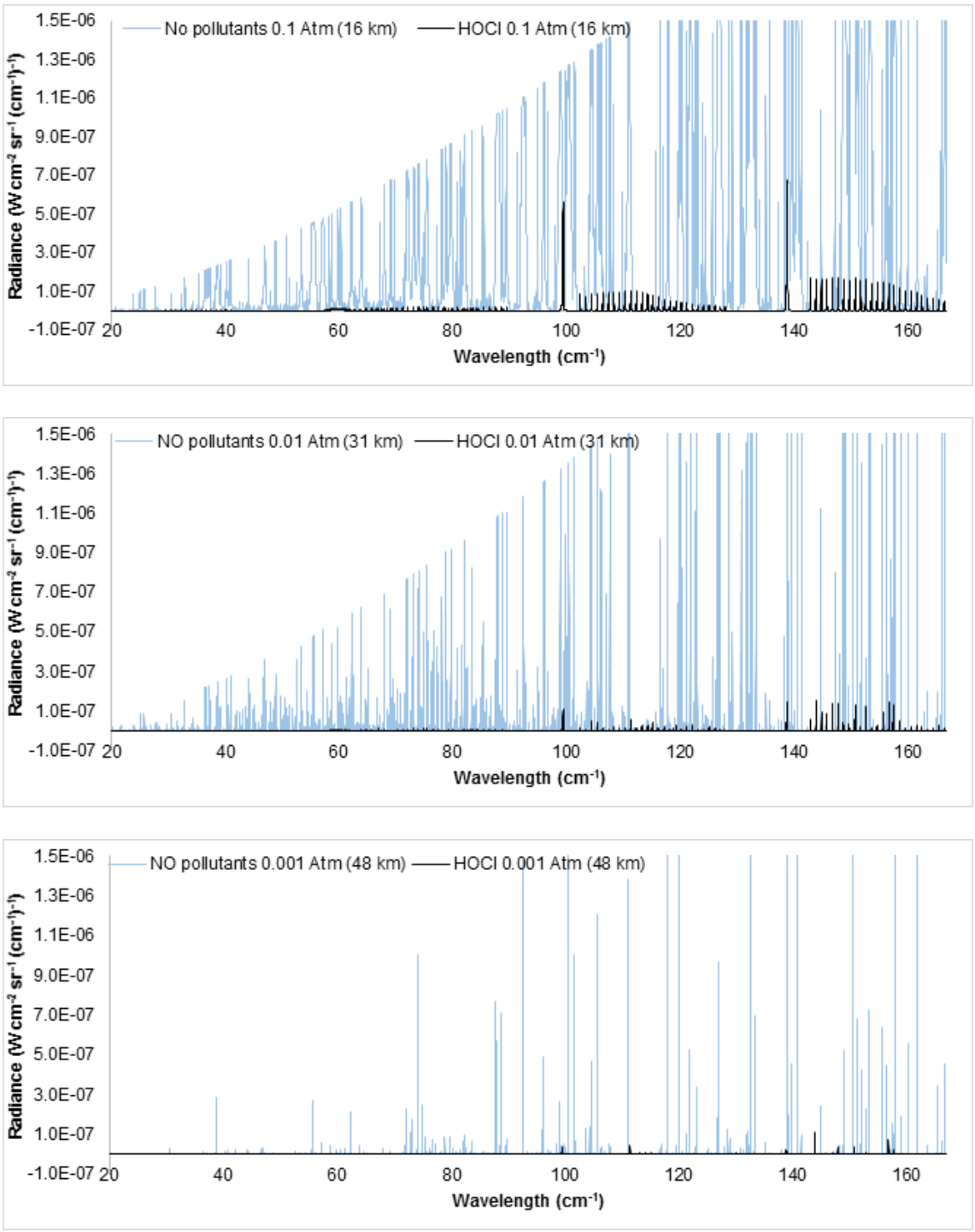

Fig. 2.11: Radiance spectrum with spectral features of the typical concentration of HOCl and the spectrum for the corresponding unpolluted atmospheres at 16, 31 and 48 km for a 10000 m homogenous path.

2.2.9 H2S

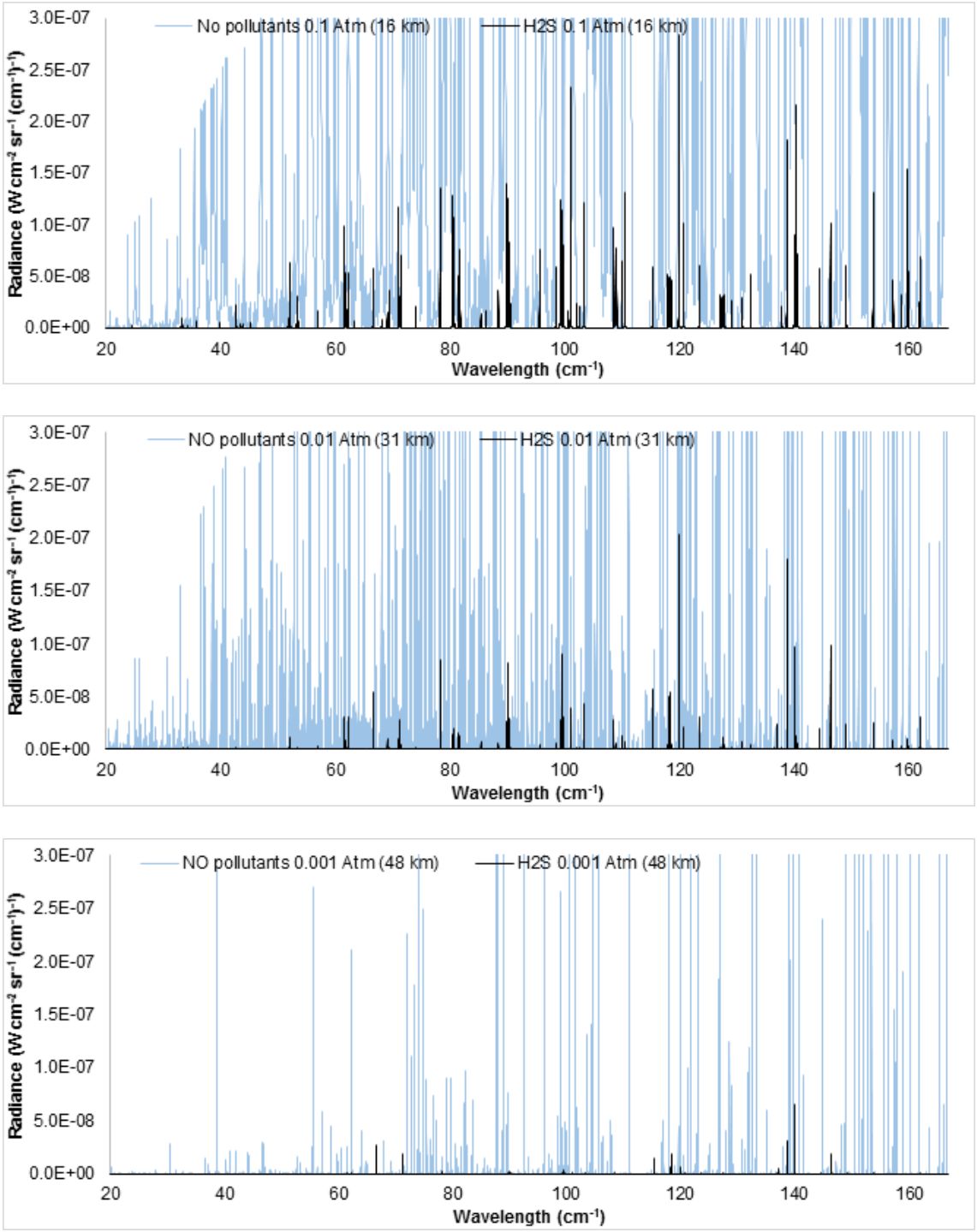

Fig. 2.12: Radiance spectrum with spectral features of the typical concentration of H2S and the spectrum for the corresponding unpolluted atmospheres at 16, 31 and 48 km for a 10000 m homogenous path.

3 Atmospheric scenario in the range 600 GHz – 5 for different geometry of observation

3.1 *Mathematical background*

If $y(x)$ is a function tabulated for n points x_i , $i = 0, \dots, n$ so that $y_i = y(x_i)$, the integral $\int y(x)\,dx$ can be written (linearly interpolating between the values at the points x_i):

$$\int_{s_0}^{s_n} y(x)\,dx = \frac{1}{2}\sum_{i=0}^{n-1}(y_i + y_{i+1})(x_{i+1} - x_i)$$

If $n = 2$ (3 levels at s_0, s_1, s_2) the formula becomes:

$$\int_{s_0}^{s_2} y(x)\,dx = \frac{1}{2}[(y_0 + y_1)(x_1 - x_0) + (y_1 + y_2)(x_2 - x_1)]$$

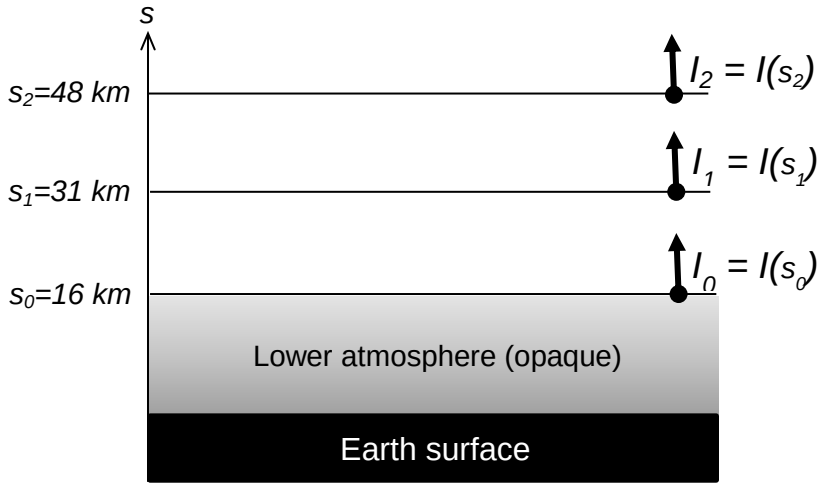

Fig. 3.1: Geometry of observation for nadir view geometry

Considering the equation introduced in par. 2.1 for a uniform medium, we have (for a linearly interpolated atmosphere between 3 levels, as in Fig. 3.1):

$$\frac{dI}{ds} = \beta_a(s)(B(T(s)) - I(s))$$

whose integral between the levels s_0 and s_n becomes:

$$I(s_n) - I(s_0) = \int_{s_0}^{s_n} \beta_a(s)(B(T(s)) - I(s))ds$$

and substituting the integral with the sum we obtain:

$$I(s_n) = I(s_0) + \frac{1}{2}\sum_{i=1}^{n}(Y_{i-1} + Y_i)(s_i - s_{1-1})$$

being: $Y_i = \beta_a(s_i)(B(T(s_i)) - I(s_i))$, $I_i = I(s_i)$, $\beta_{a_i} = \beta_a(s_i)$ and $B(T(s_i)) = B_i$.
In the following paragraphs we'll consider a simple, 3 level model atmosphere. The equations became then:

$$I_0 = I(s_0)$$

$$I_1 = I_0 + \frac{1}{2}\{[\beta_{a_0}(B_0 - I_0) + \beta_{a_1}(B_1 - I_1)](s_1 - s_0)\}$$

$$I_2 = I_0 + \frac{1}{2}\{[\beta_{a_0}(B_0 - I_0) + \beta_{a_1}(B_1 - I_1)](s_1 - s_0) + [\beta_{a_1}(B_1 - I_1) + \beta_{a_2}(B_2 - I_2)](s_2 - s_1)\} =$$

$$= I_1 + \frac{1}{2}\{[\beta_{a_1}(B_1 - I_1) + \beta_{a_2}(B_2 - I_2)](s_2 - s_1)\}$$

3.2 *Nadir view from top of atmosphere: linearly interpolated levels model*

The value for I_0 is given by the radiance reaching the level s_0 (for example the radiance emitted by ground and lower atmospheric layers or the power emitted by an active source). The solution for the observed radiance I_2, as a function of the radiance I_o is then (with the same signs as in Fig. 3.1):

$$I_1 = I_0 + \frac{1}{2}\left[\beta_{a_0}(B_0 - I_0) + \beta_{a_1}(B_1 - I_1)\right](s_1 - s_0)$$
$$I_2 = I_1 + \frac{1}{2}\left[\beta_{a_1}(B_1 - I_1) + \beta_{a_2}(B_2 - I_2)\right](s_2 - s_1)$$

Solving the system and defining:

$$\Delta s_1 = s_1 - s_0$$
$$\Delta s_2 = s_2 - s_1$$

we calculate I_1 and I_2 as:

$$I_1 = \frac{\left(2 - \beta_{a_0}\Delta s_1\right)I_0 + \Delta s_1\left(\beta_{a_1}B_1 + \beta_{a_0}B_0\right)}{\beta_{a_1}\Delta s_1 + 2}$$

$$I_2 = \frac{\left[\left(\beta_{a_0}\Delta s_1 - 2\right)\beta_{a_1}\Delta s_2 - 2\beta_{a_0}\Delta s_1 + 4\right]I_0 + \left(\beta_{a_1}\Delta s_1 + 2\right)\beta_{a_2}\Delta s_2 B_2 + 2(\Delta s_2 + \Delta s_1)\beta_{a_1}B_1 + \left(2 - \beta_{a_1}\Delta s_2\right)\beta_{a_0}\Delta s_1 B_0}{\left(\beta_{a_1}\Delta s_1 + 2\right)\beta_{a_2}\Delta s_2 + 2\beta_{a_1}\Delta s_1 + 4}$$

or, also:

$$I_2 = \alpha_g I_0 + \alpha_2 B_2 + \alpha_1 B_1 + \alpha_0 B_0$$

with:

$$\alpha_g = \frac{\left(\beta_{a_0}\Delta s_1 - 2\right)\beta_{a_1}\Delta s_2 - 2\beta_{a_0}\Delta s_1 + 4}{\left(\beta_{a_1}\Delta s_1 + 2\right)\beta_{a_2}\Delta s_2 + 2\beta_{a_1}\Delta s_1 + 4}$$
$$\alpha_0 = \frac{\left(2 - \beta_{a_1}\Delta s_2\right)\beta_{a_0}\Delta s_1}{\left(\beta_{a_1}\Delta s_1 + 2\right)\beta_{a_2}\Delta s_2 + 2\beta_{a_1}\Delta s_1 + 4}$$
$$\alpha_1 = \frac{2(\Delta s_2 + \Delta s_1)\beta_{a_1}}{\left(\beta_{a_1}\Delta s_1 + 2\right)\beta_{a_2}\Delta s_2 + 2\beta_{a_1}\Delta s_1 + 4}$$

$$\alpha_2 = \frac{\left(\beta_{a_1}\Delta s_1 + 2\right)\beta_{a_2}\Delta s_2}{\left(\beta_{a_1}\Delta s_1 + 2\right)\beta_{a_2}\Delta s_2 + 2\beta_{a_1}\Delta s_1 + 4}$$

The radiance I_2 observed in nadir direction (i.e. observing ground from the top of atmosphere) has been calculated for a stratified *unpolluted* atmosphere. For the layers 0 – 3 the values used are from the atmospheres described in par. 2.2 for the three different altitudes.

The corresponding radiance has been calculated also for different *polluted* atmospheres, in which the absorption coefficient of each pollutant has been added to the absorption coefficient of the unpolluted atmosphere, as in par. 2.2.1 - 2.2.9. In this way, each atmosphere has an observed radiance spectrum as a function of each pollutant.

3.2.1 NO2

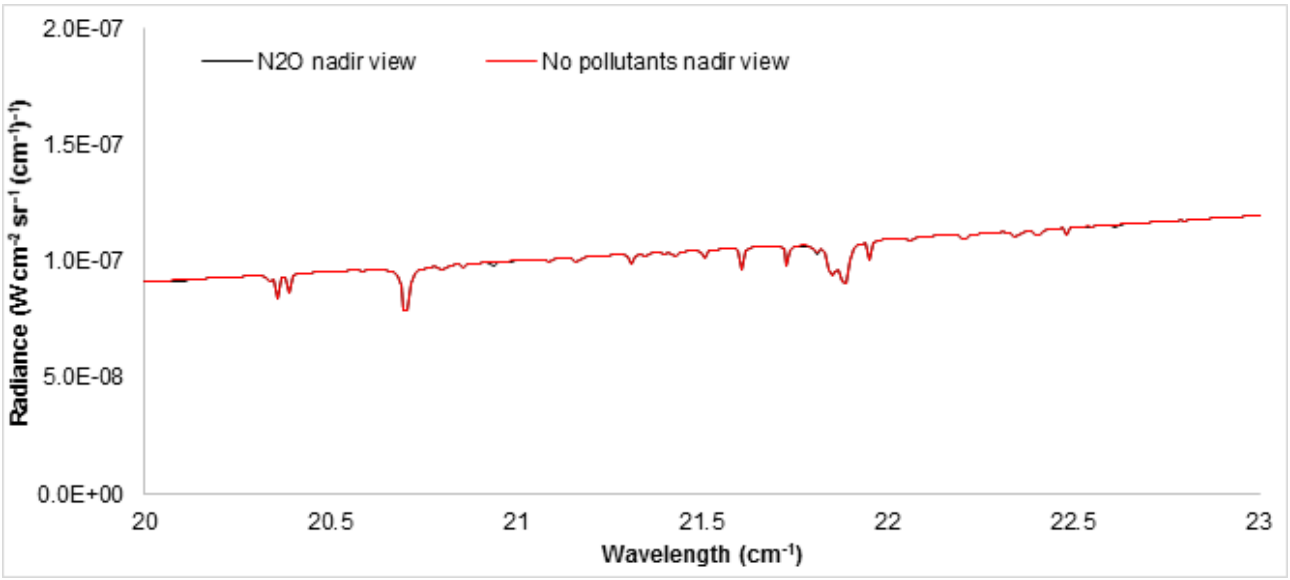

Fig. 3.2: Radiance spectrum with spectral features of the typical concentration of N2O for a nadir (towards ground) view in a 3 level linearly interpolated atmosphere introduced in par. 2.2.

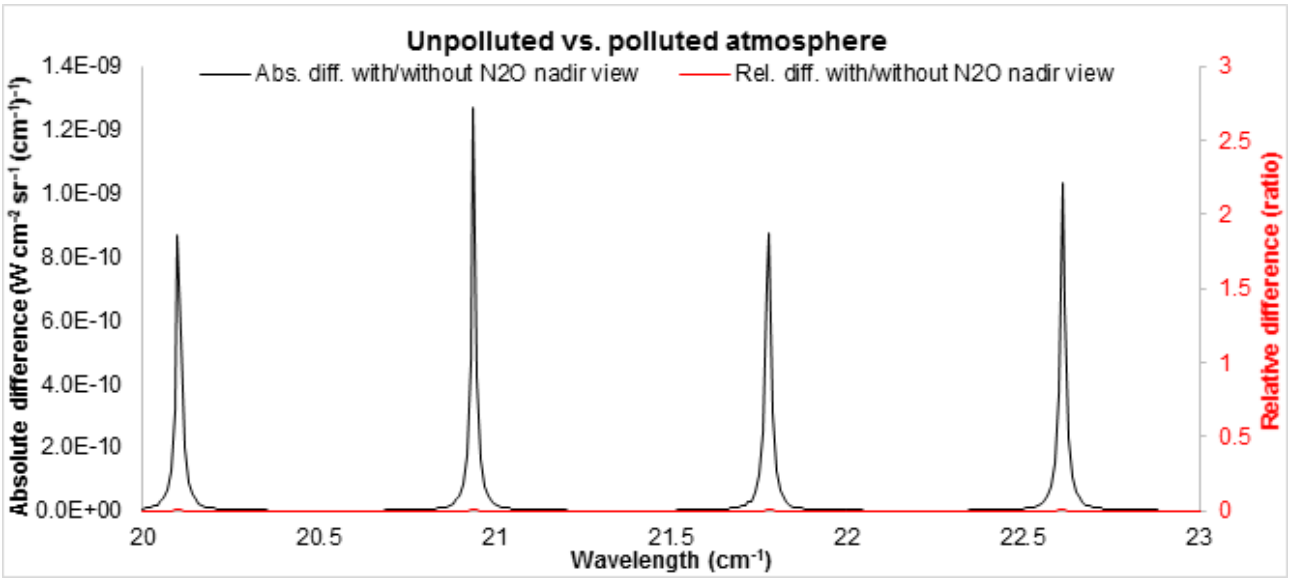

Fig. 3.3: Absolute and relative difference for the radiance spectrum of the unpolluted atmosphere introduced in par. 2.2 and the same atmosphere with the typical concentration of N2O.

3.2.2 CO

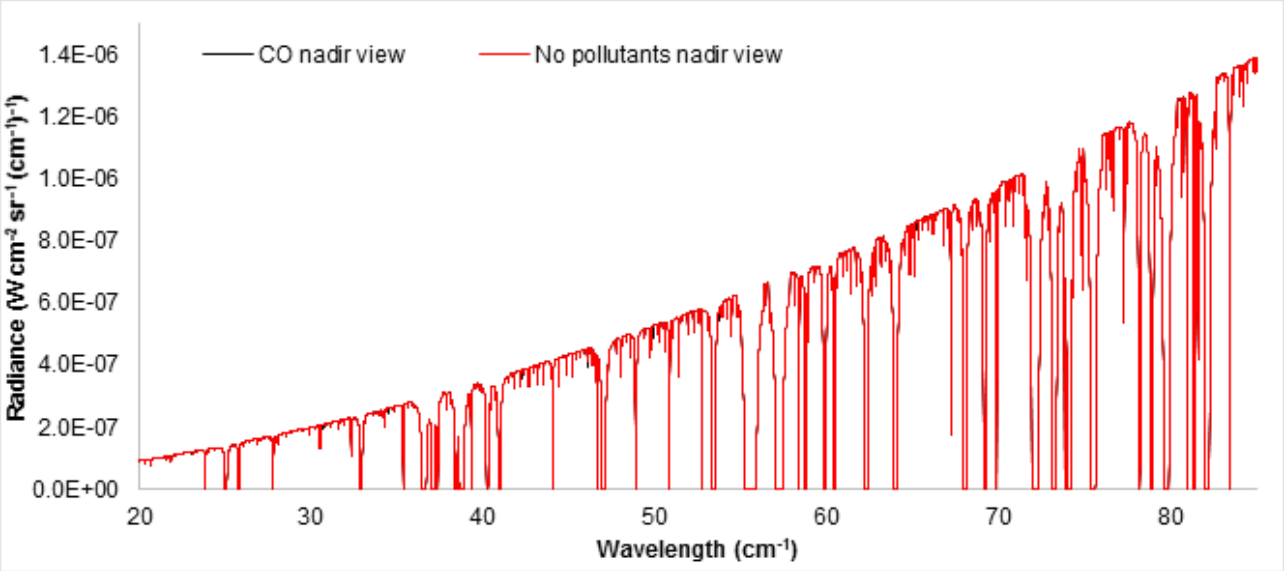

Fig. 3.4: Radiance spectrum with spectral features of the typical concentration of CO for a nadir (towards ground) view in a 3 level linearly interpolated atmosphere introduced in par. 2.2

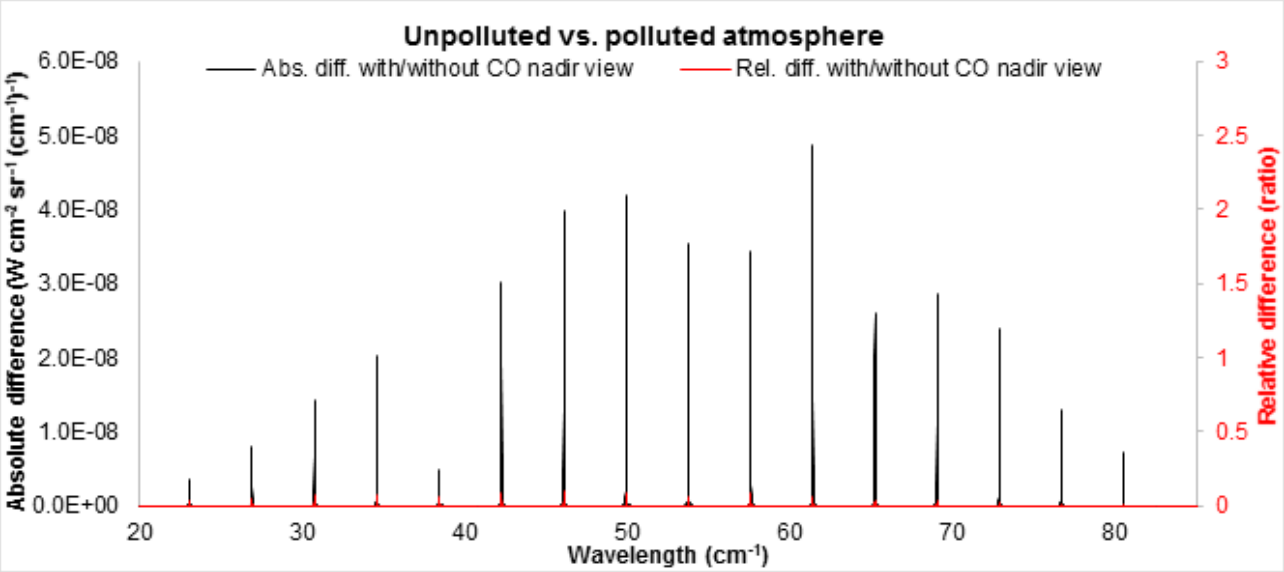

Fig. 3.5: Absolute and relative difference for the radiance spectrum of the unpolluted atmosphere introduced in par. 2.2 and the same atmosphere with the typical concentration of CO.

3.2.3 SO2

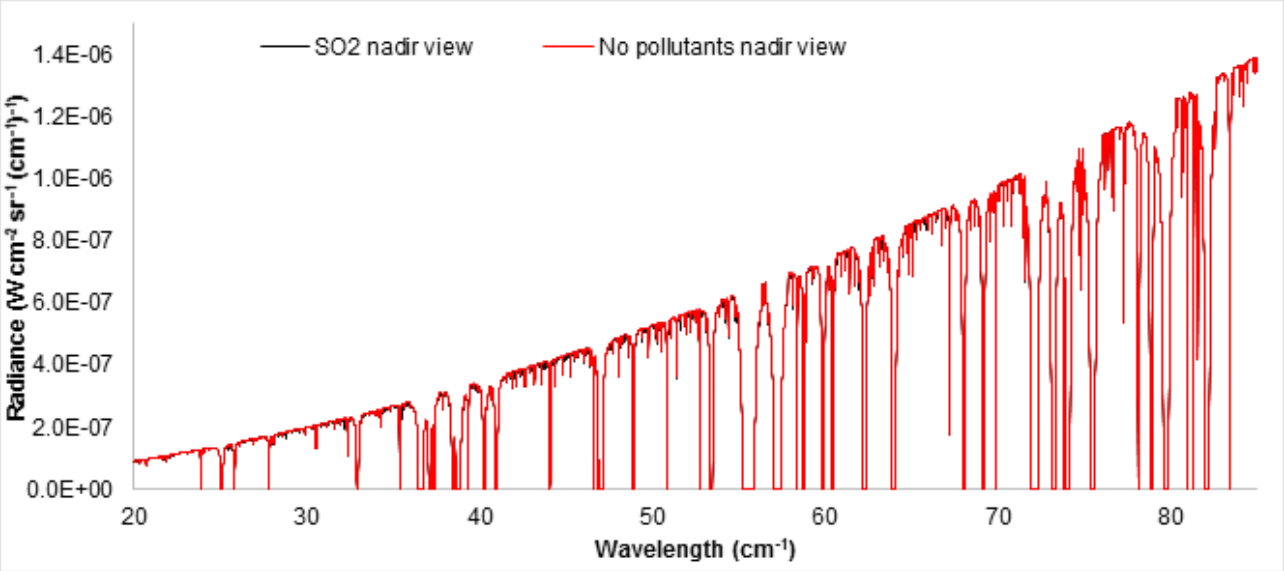

Fig. 3.6: Radiance spectrum with spectral features of the typical concentration of SO2 for a nadir (towards ground) view in a 3 level linearly interpolated atmosphere introduced in par. 2.2

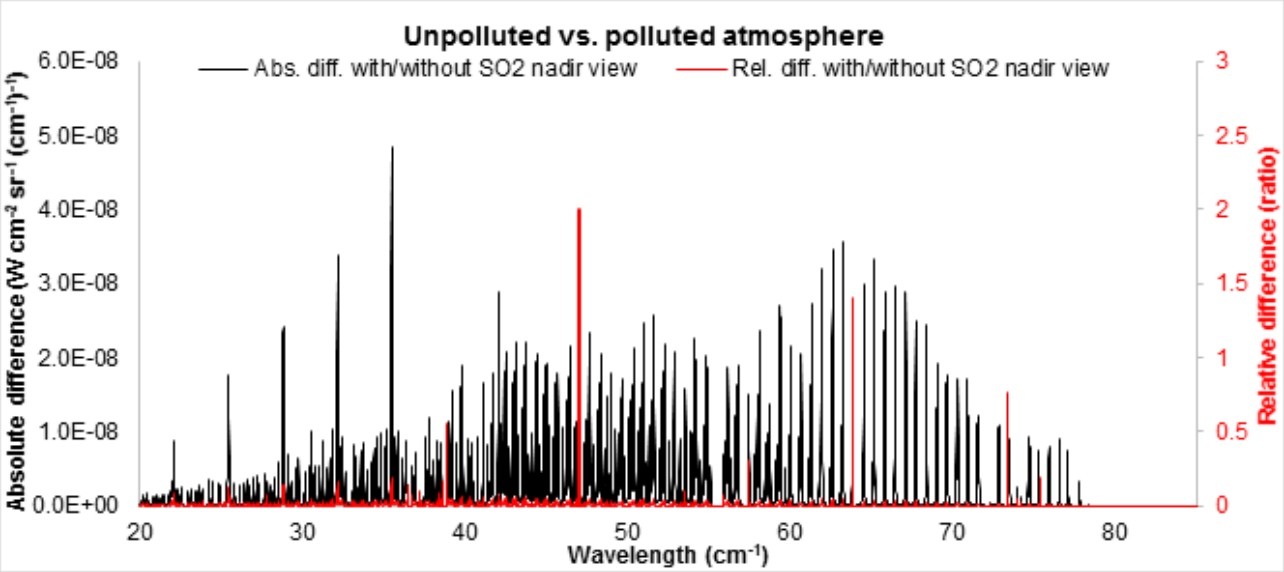

Fig. 3.7: Absolute and relative difference for the radiance spectrum of the unpolluted atmosphere introduced in par. 2.2 and the same atmosphere with the typical concentration of SO2.

3.2.4 NH3

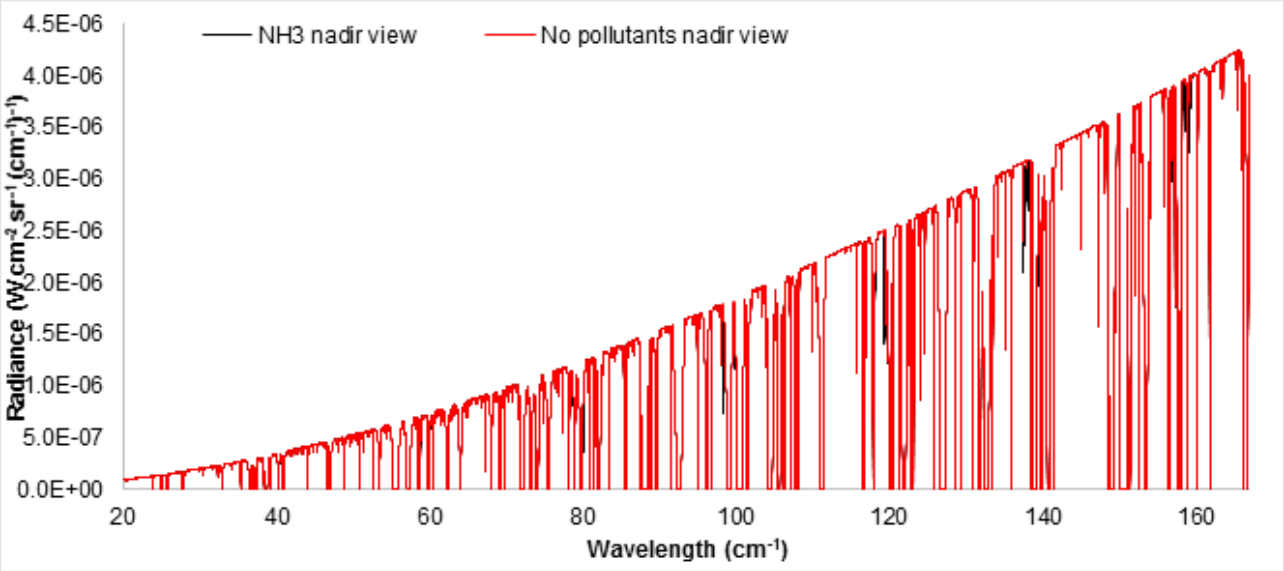

Fig. 3.8: Radiance spectrum with spectral features of the typical concentration of NH3 for a nadir (towards ground) view in a 3 level linearly interpolated atmosphere introduced in par. 2.2

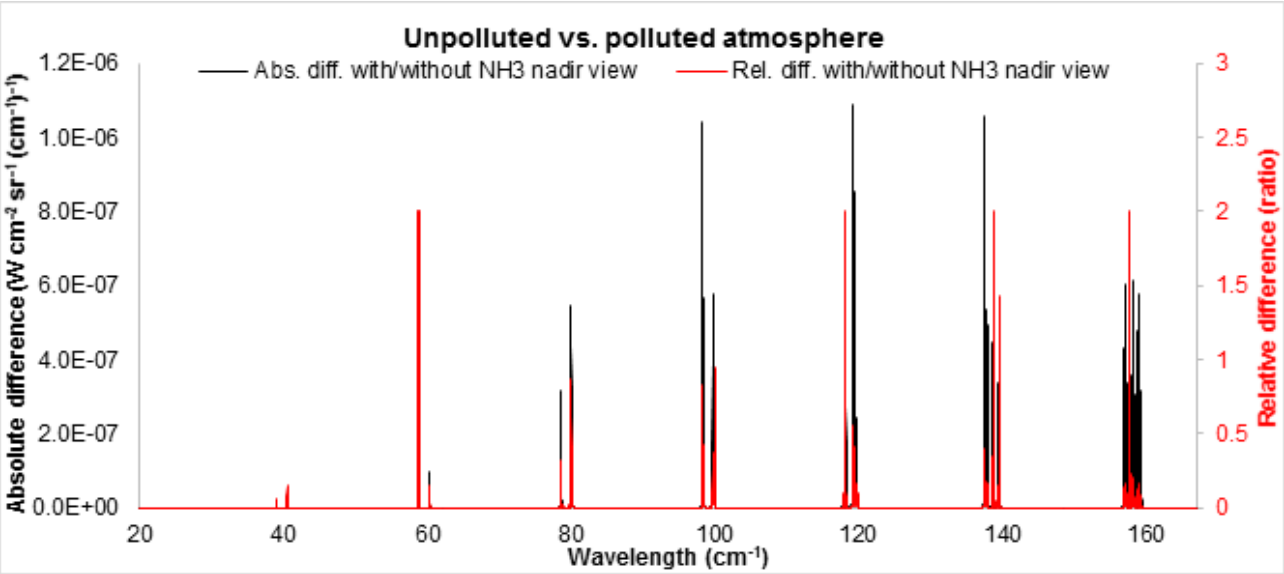

Fig. 3.9: Absolute and relative difference for the radiance spectrum of the unpolluted atmosphere introduced in par. 2.2 and the same atmosphere with the typical concentration of NH3.

3.2.5 OH

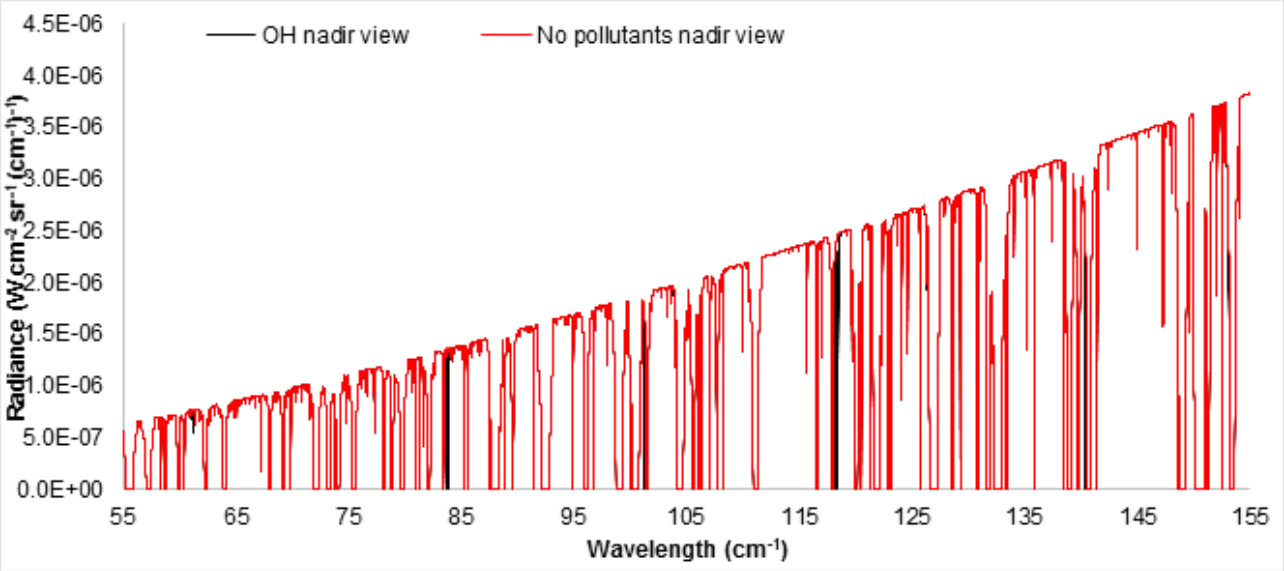

Fig. 3.10: Radiance spectrum with spectral features of the typical concentration of OH for a nadir (towards ground) view in a 3 level linearly interpolated atmosphere introduced in par. 2.2

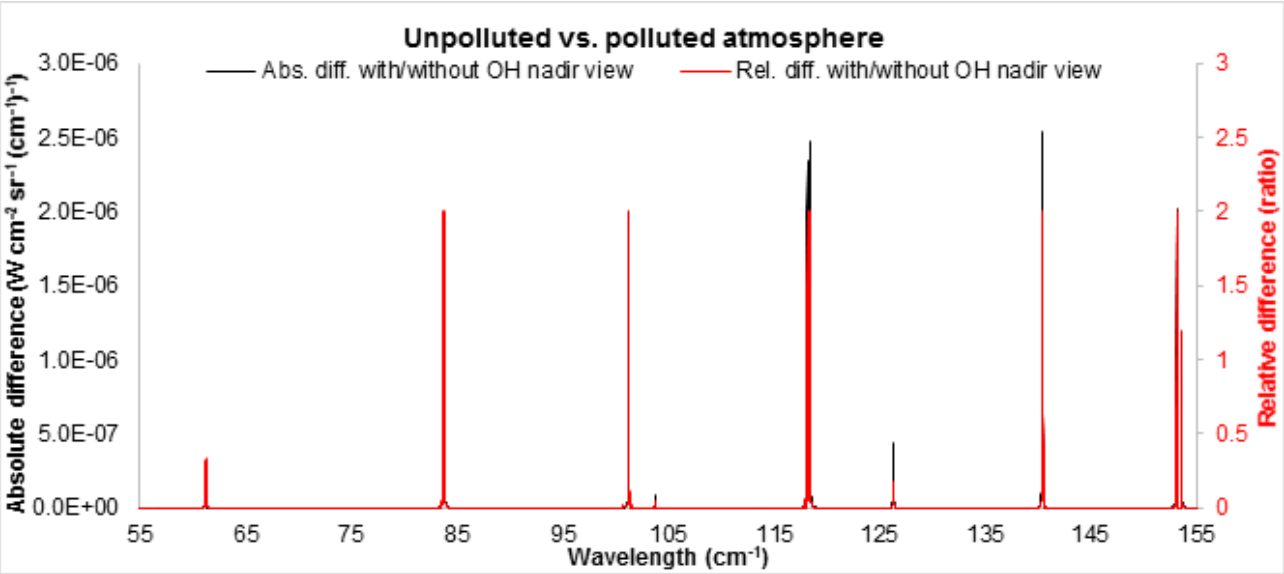

Fig. 3.11: Absolute and relative difference for the radiance spectrum of the unpolluted atmosphere introduced in par. 2.2 and the same atmosphere with the typical concentration of OH.

3.2.6 HCl

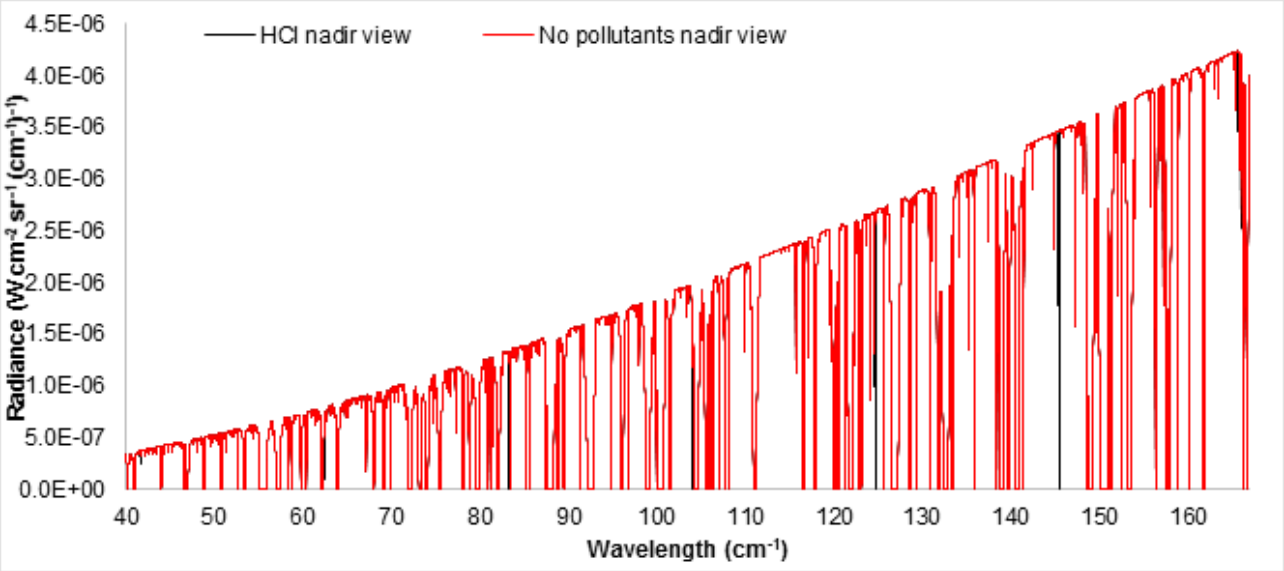

Fig. 3.12: Radiance spectrum with spectral features of the typical concentration of HCl for a nadir (towards ground) view in a 3 level linearly interpolated atmosphere introduced in par. 2.2

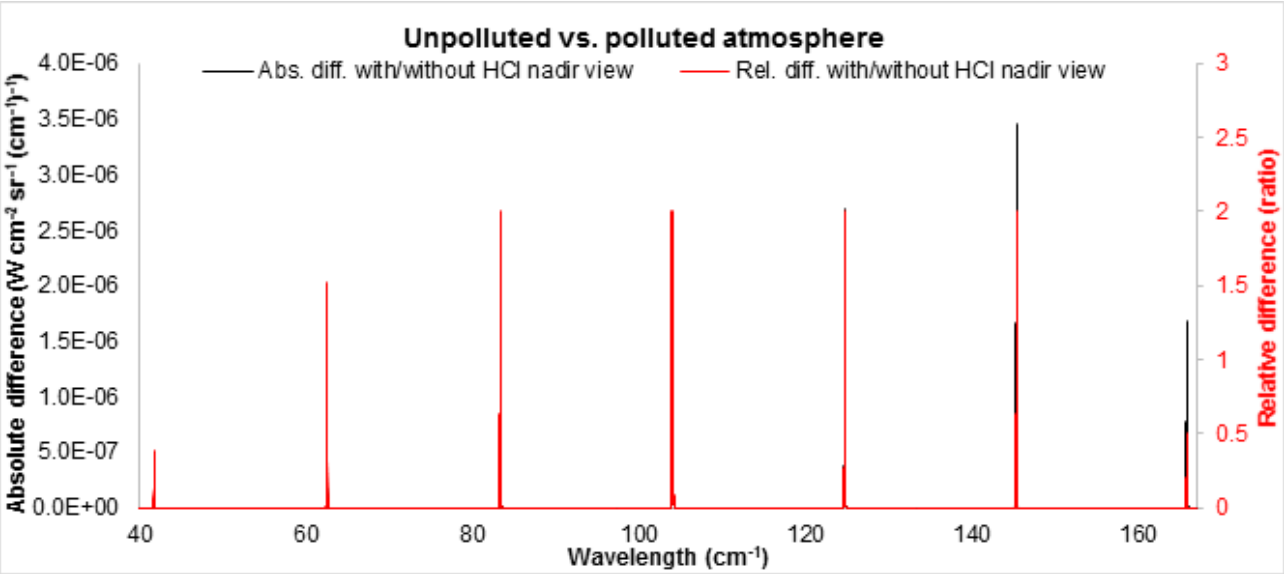

Fig. 3.13: Absolute and relative difference for the radiance spectrum of the unpolluted atmosphere introduced in par. 2.2 and the same atmosphere with the typical concentration of HCl.

3.2.7 H2CO

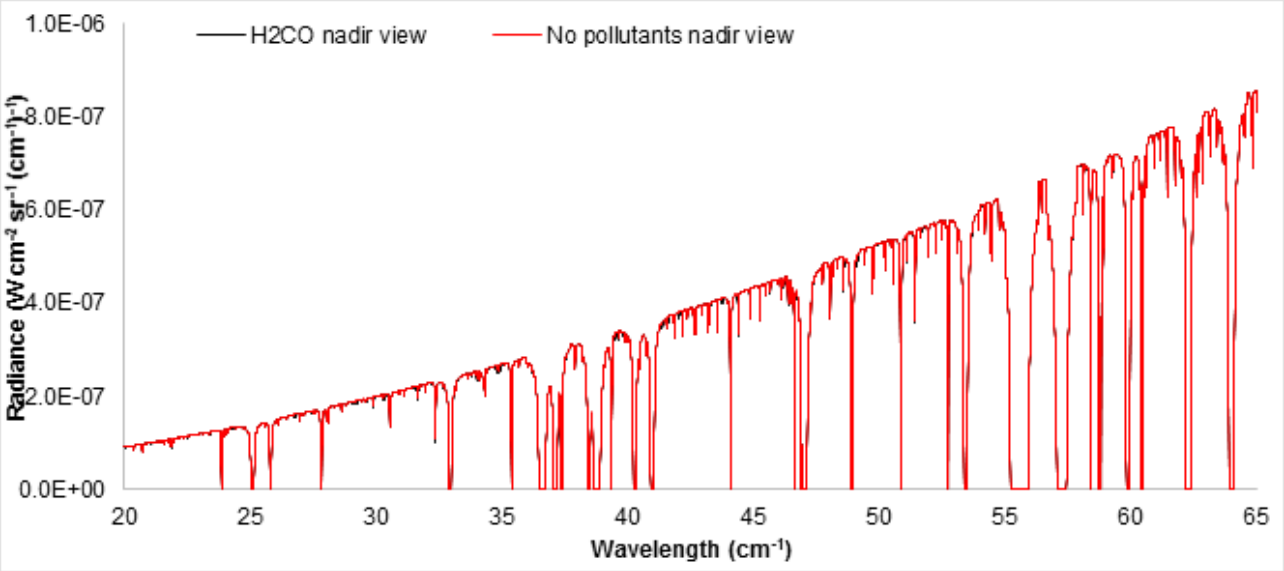

Fig. 3.14: Radiance spectrum with spectral features of the typical concentration of H2CO for a nadir (towards ground) view in a 3 level linearly interpolated atmosphere introduced in par. 2.2

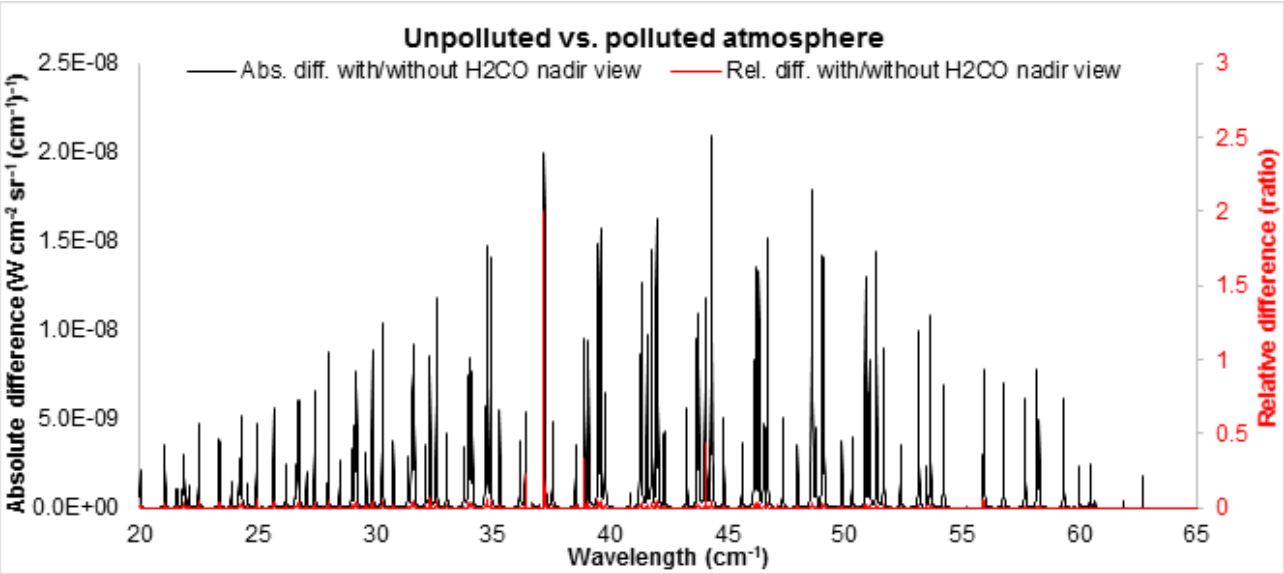

Fig. 3.15: Absolute and relative difference for the radiance spectrum of the unpolluted atmosphere introduced in par. 2.2 and the same atmosphere with the typical concentration of H2CO.

3.2.8 HOCl

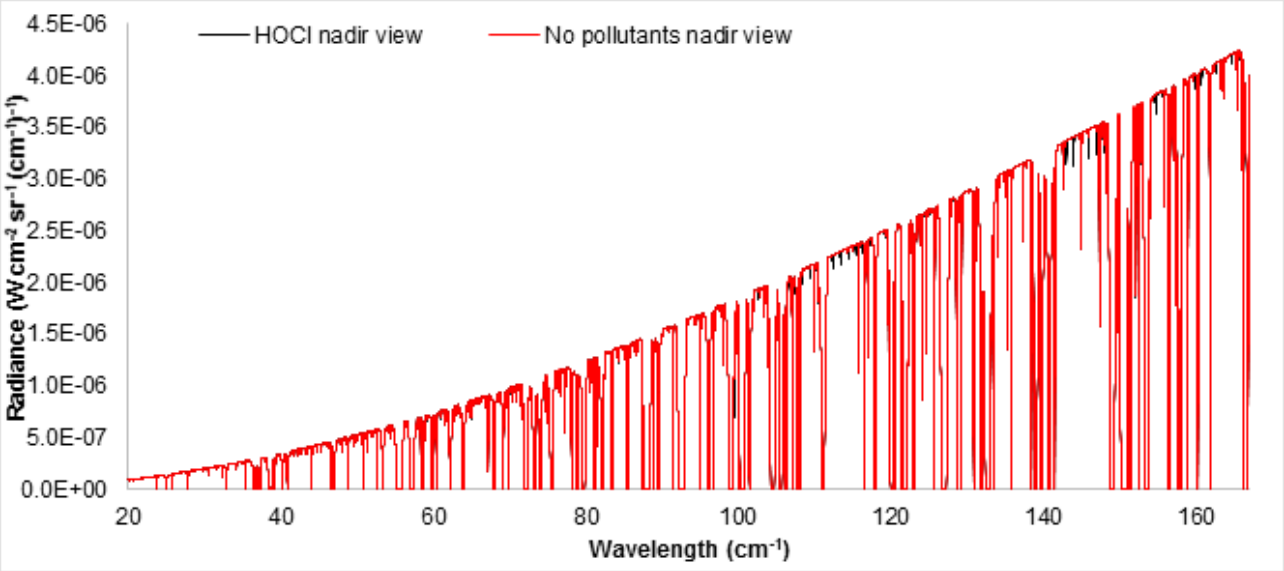

Fig. 3.16: Radiance spectrum with spectral features of the typical concentration of HOCl for a nadir (towards ground) view in a 3 level linearly interpolated atmosphere introduced in par. 2.2

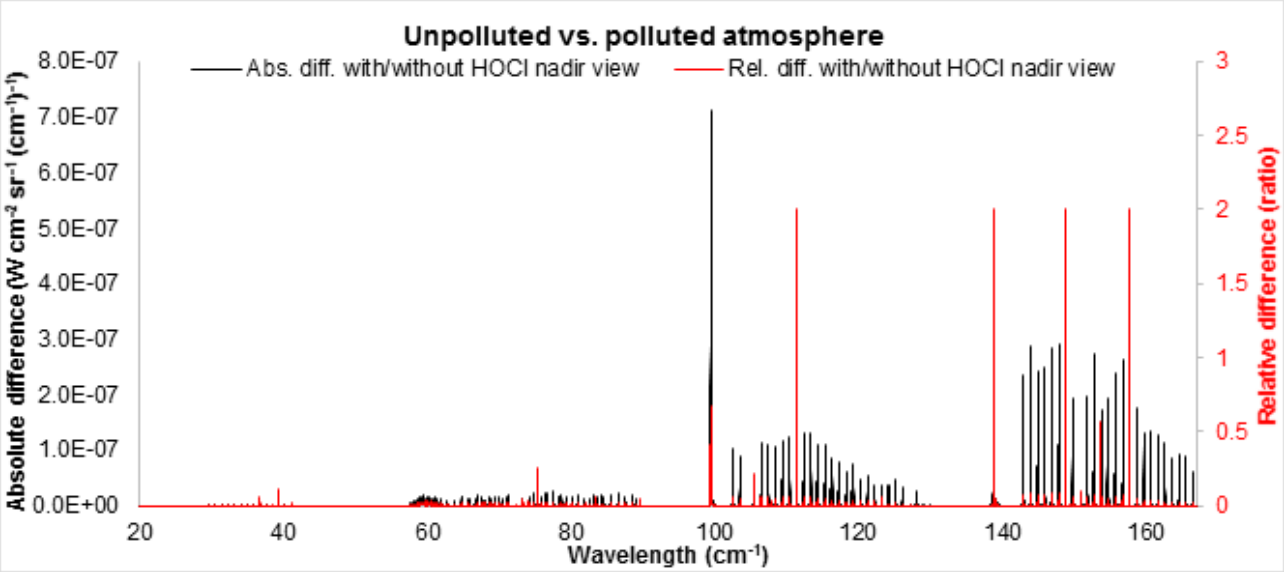

Fig. 3.17: Absolute and relative difference for the radiance spectrum of the unpolluted atmosphere introduced in par. 2.2 and the same atmosphere with the typical concentration of HOCl.

3.2.9 H2S

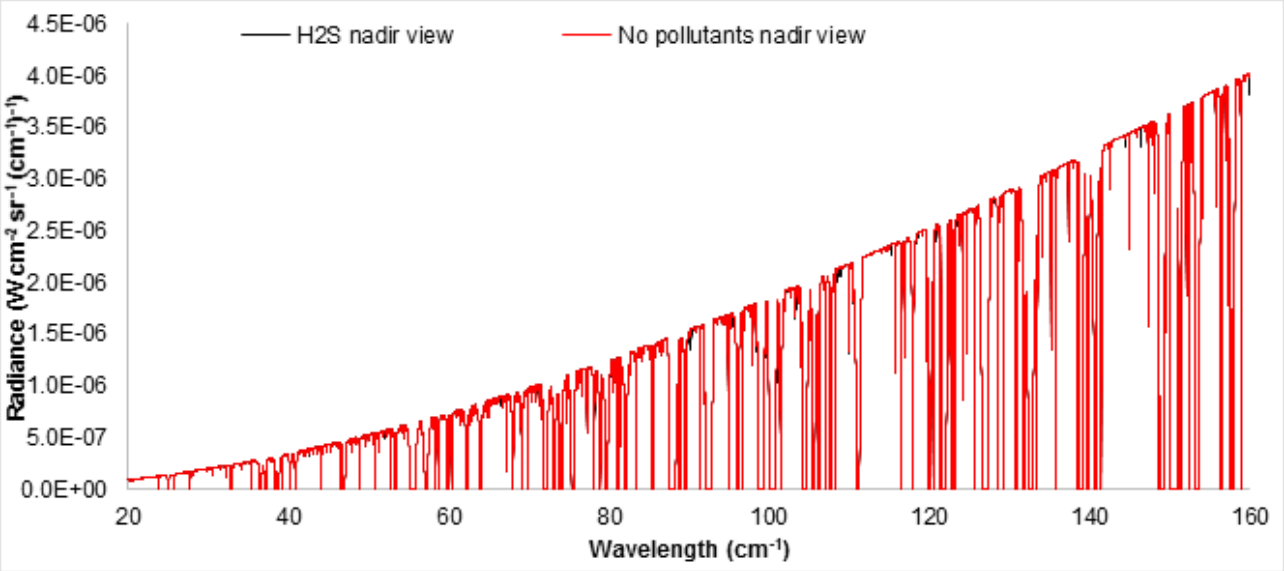

Fig. 3.18: Radiance spectrum with spectral features of the typical concentration of H2S for a nadir (towards ground) view in a 3 level linearly interpolated atmosphere introduced in par. 2.2

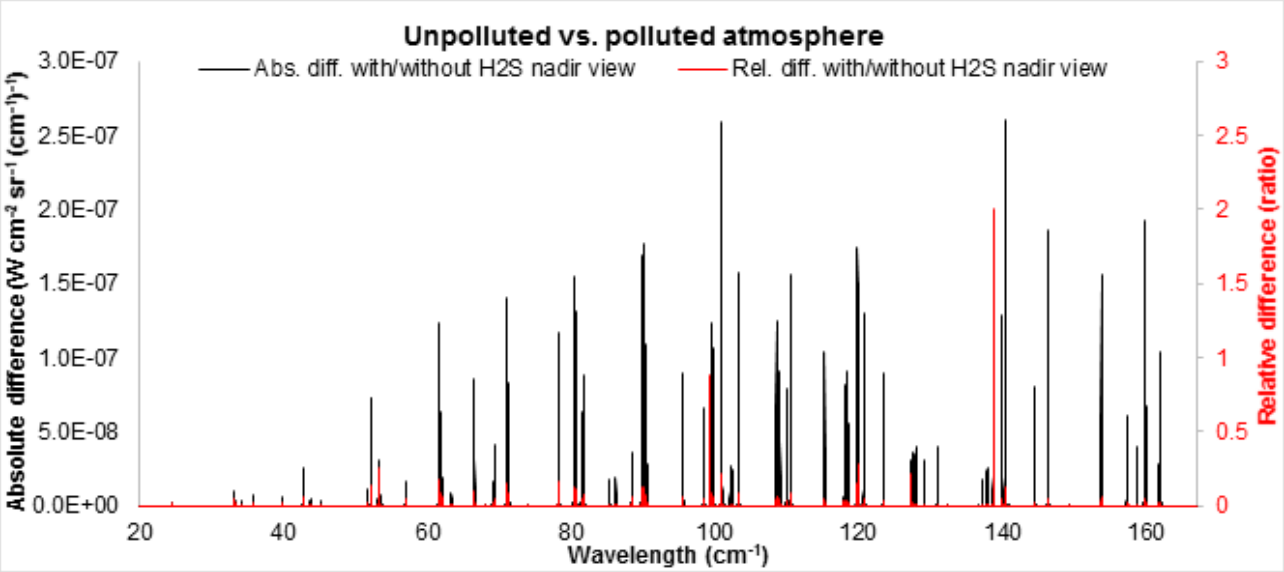

Fig. 3.19: Absolute and relative difference for the radiance spectrum of the unpolluted atmosphere introduced in par. 2.2 and the same atmosphere with the typical concentration of H2S.

3.3 *Zenith view from lower atmosphere: linearly interpolated level model*

We calculate $I'_0 = -I_0$ (down-welling radiance received at the lower level) as a function of $I'_1 = -I_1$ and $I'_2 = -I_2$ using the same formula:

$$I'_1 = \frac{\left(2 - \beta_{a_0}\Delta s_1\right)I'_2 - \Delta s_1\left(\beta_{a_0}B_0 + \beta_{a_1}B_1\right)}{\beta_{a_1}\Delta s_1 + 2}$$

$$I'_0 = \\ = \frac{\left[\left(\beta_{a_0}\Delta s_1 - 2\right)\beta_{a_1}\Delta s_2 - 2\beta_{a_0}\Delta s_1 + 4\right]I'_2 - \left(\beta_{a_1}\Delta s_1 + 2\right)\beta_{a_2}\Delta s_2 B_2 - 2(\Delta s_2 + \Delta s_1)\beta_{a_1}B_1 - \left(2 - \beta_{a_1}\Delta s_2\right)\beta_{a_0}\Delta s_1 B_0}{\left(\beta_{a_1}\Delta s_1 + 2\right)\beta_{a_2}\Delta s_2 + 2\beta_{a_1}\Delta s_1 + 4}$$

and, setting $I'_2 = 0$ (no source term from space), we obtain:

$$I'_0 = -\frac{\left(\beta_{a_1}\Delta s_1 + 2\right)\beta_{a_2}\Delta s_2 B_2 + 2(\Delta s_2 + \Delta s_1)\beta_{a_1}B_1 + \left(2 - \beta_{a_1}\Delta s_2\right)\beta_{a_0}\Delta s_1 B_0}{\left(\beta_{a_1}\Delta s_1 + 2\right)\beta_{a_2}\Delta s_2 + 2\beta_{a_1}\Delta s_1 + 4}$$

where the minus sign is due to the direction of the system of reference (i.e. the radiance is received oppositely to the vertical axis).

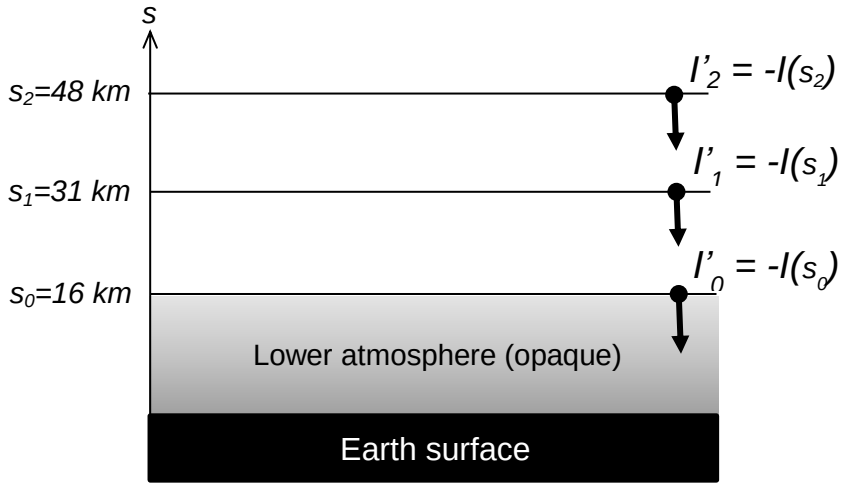

Fig. 3.20: Geometry of observation for nadir view geometry

For the radiance I'_0 and for a zenith view (i.e. observing the top of atmosphere from s_0) the same charts as in par.3.2 have been evaluated, comparing the radiance from an unpolluted atmosphere with the radiance of a polluted ones for each pollutant.

3.3.1 N2O

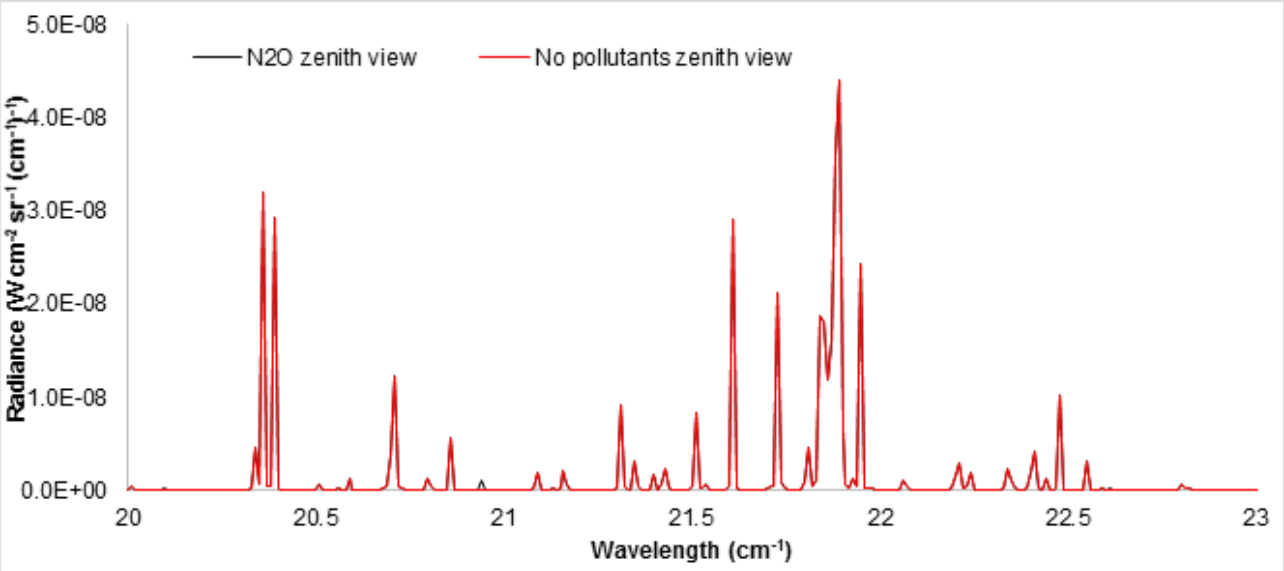

Fig. 3.21: Radiance spectrum with spectral features of the typical concentration of N2O for a zenith (towards the top of atmosphere) view in a 3 level linearly interpolated atmosphere introduced in par. 2.2

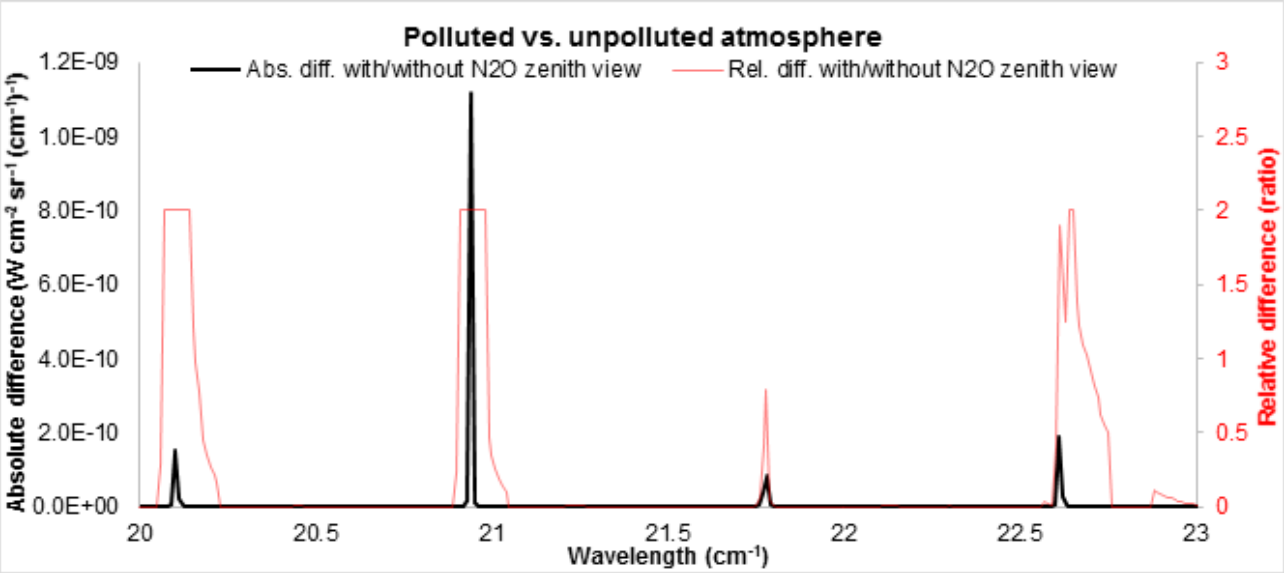

Fig. 3.22: Absolute and relative difference for the radiance spectrum of the atmosphere introduced in par. 2.2 with the typical concentration of N2O and the corresponding unpolluted atmosphere.

3.3.2 CO

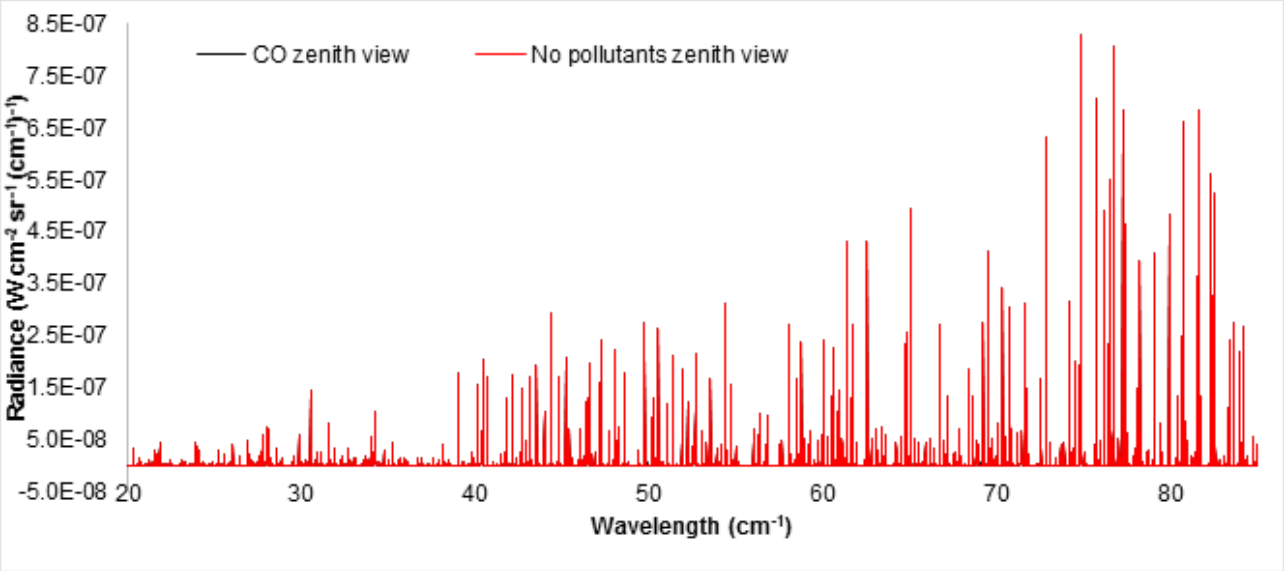

Fig. 3.23: Radiance spectrum with spectral features of the typical concentration of CO for a zenith (towards the top of atmosphere) view in a 3 level linearly interpolated atmosphere introduced in par. 2.2

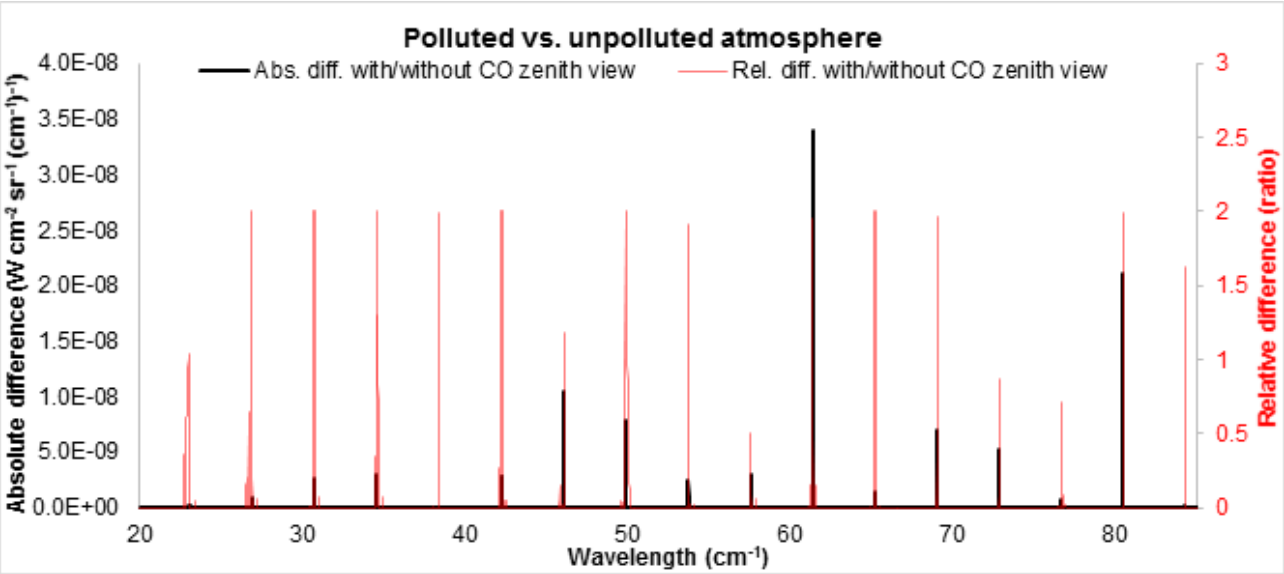

Fig. 3.24: Absolute and relative difference for the radiance spectrum of the atmosphere introduced in par. 2.2 with the typical concentration of CO and the corresponding unpolluted atmosphere.

3.3.3 SO2

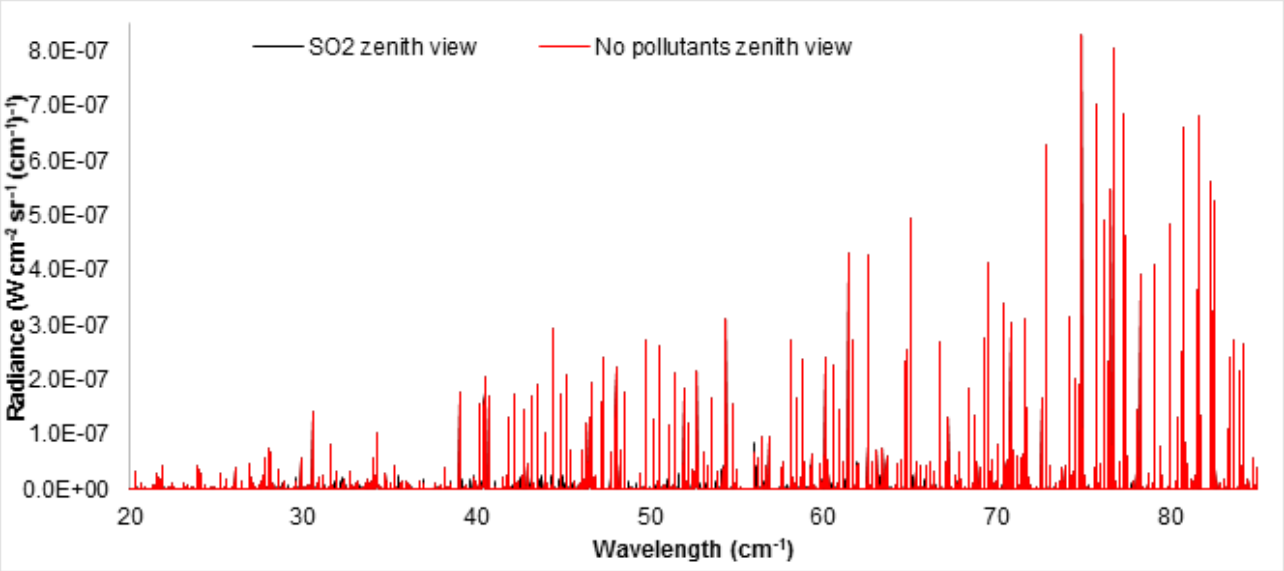

Fig. 3.25: Radiance spectrum with spectral features of the typical concentration of SO2 for a zenith (towards the top of atmosphere) view in a 3 level linearly interpolated atmosphere introduced in par. 2.2

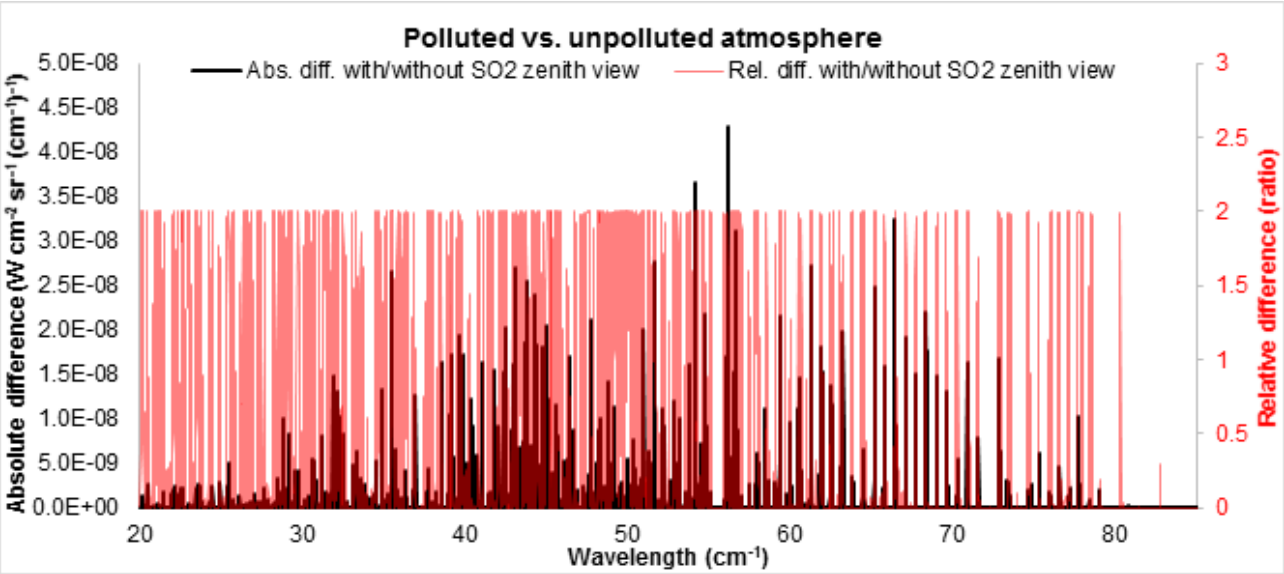

Fig. 3.26: Absolute and relative difference for the radiance spectrum of the atmosphere introduced in par. 2.2 with the typical concentration of SO2 and the corresponding unpolluted atmosphere.

3.3.4 NH3

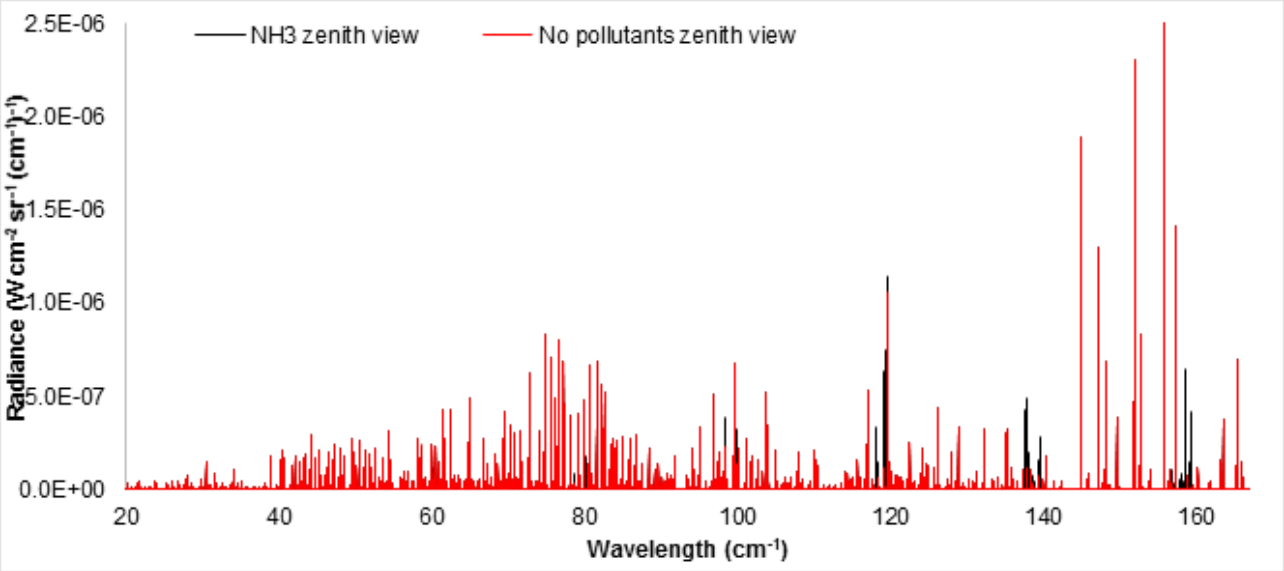

Fig. 3.27: Radiance spectrum with spectral features of the typical concentration of NH3 for a zenith (towards the top of atmosphere) view in a 3 level linearly interpolated atmosphere introduced in par. 2.2

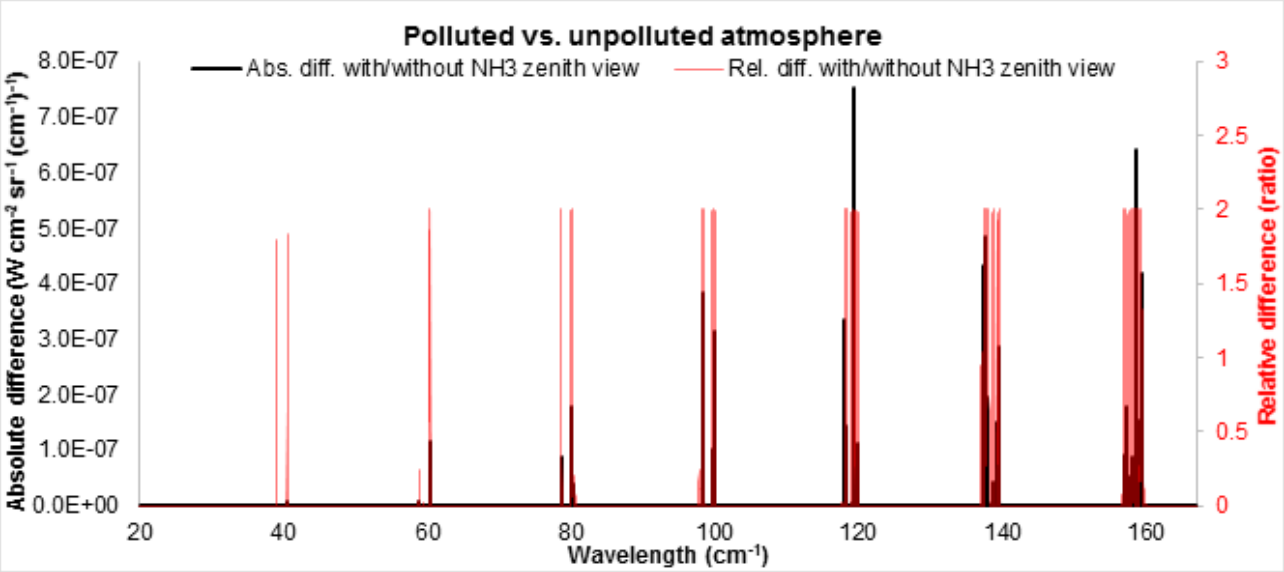

Fig. 3.28: Absolute and relative difference for the radiance spectrum of the atmosphere introduced in par. 2.2 with the typical concentration of NH3 and the corresponding unpolluted atmosphere.

3.3.5 OH

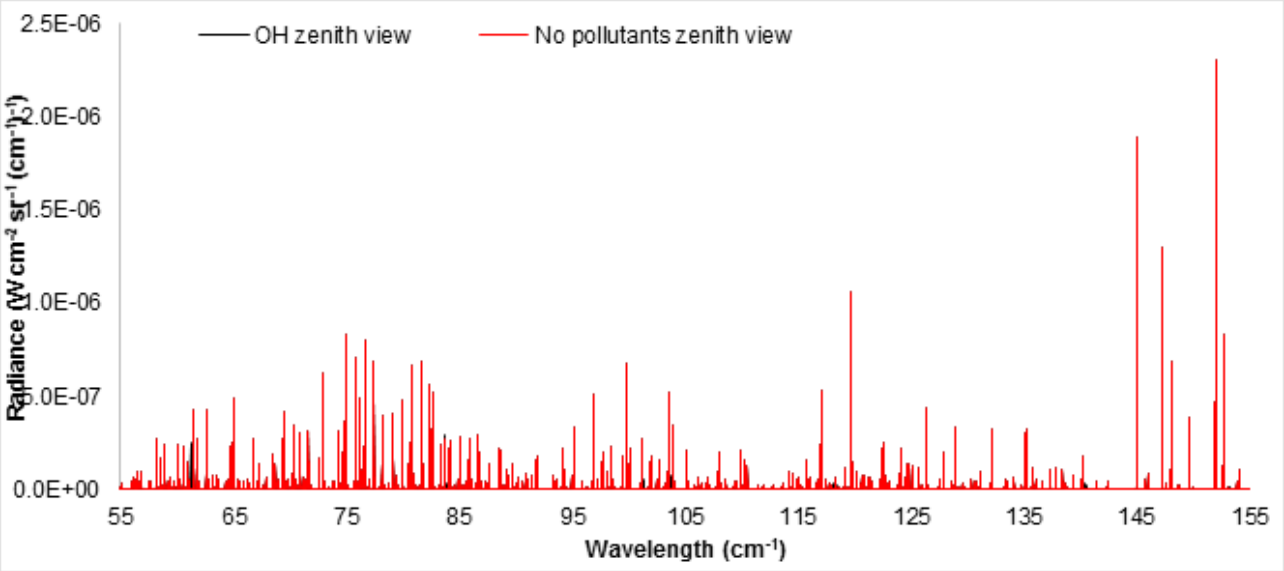

Fig. 3.29: Radiance spectrum with spectral features of the typical concentration of OH for a zenith (towards the top of atmosphere) view in a 3 level linearly interpolated atmosphere introduced in par. 2.2

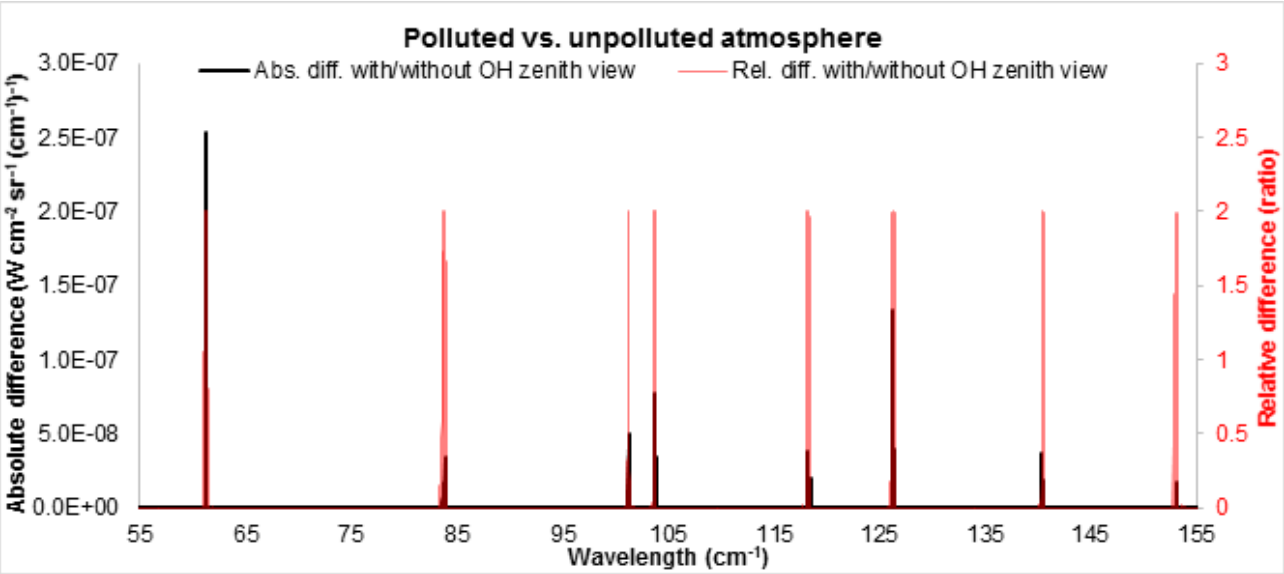

Fig. 3.30: Absolute and relative difference for the radiance spectrum of the atmosphere introduced in par. 2.2 with the typical concentration of OH and the corresponding unpolluted atmosphere.

3.3.6 HCl

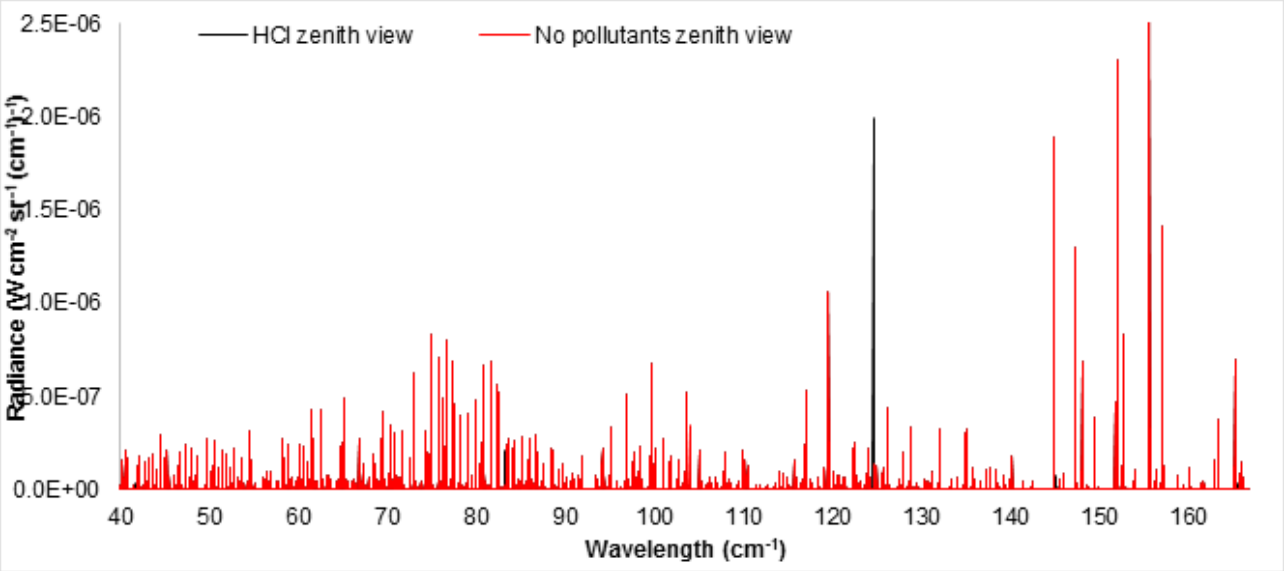

Fig. 3.31: Radiance spectrum with spectral features of the typical concentration of HCl for a zenith (towards the top of atmosphere) view in a 3 level linearly interpolated atmosphere introduced in par. 2.2

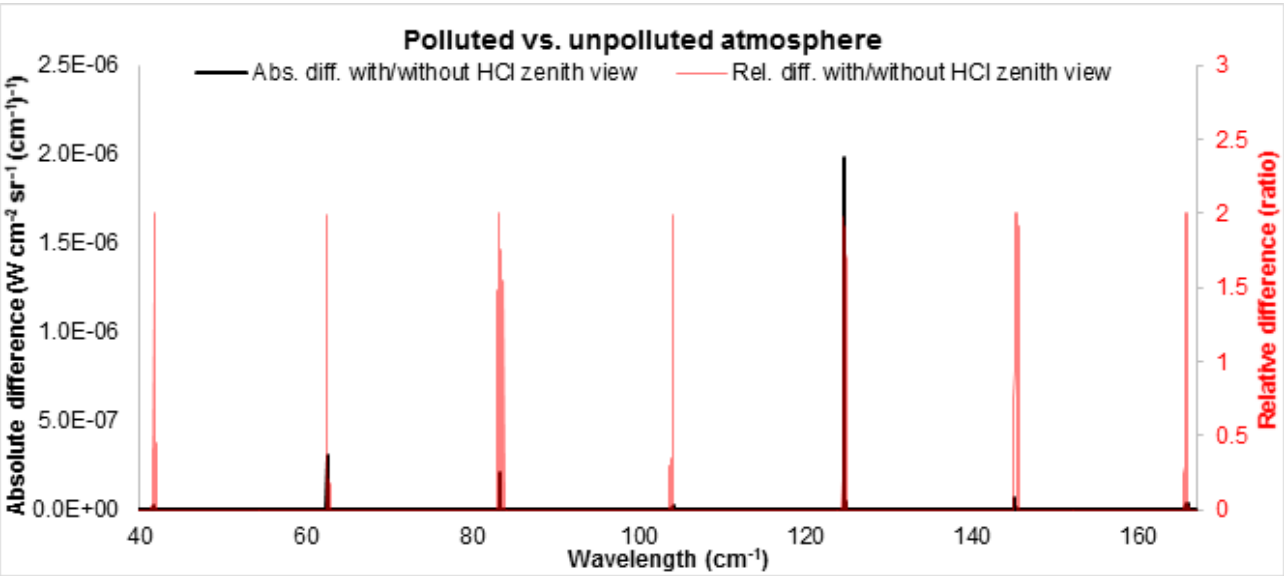

Fig. 3.32: Absolute and relative difference for the radiance spectrum of the atmosphere introduced in par. 2.2 with the typical concentration of HCl and the corresponding unpolluted atmosphere.

3.3.7 H2CO

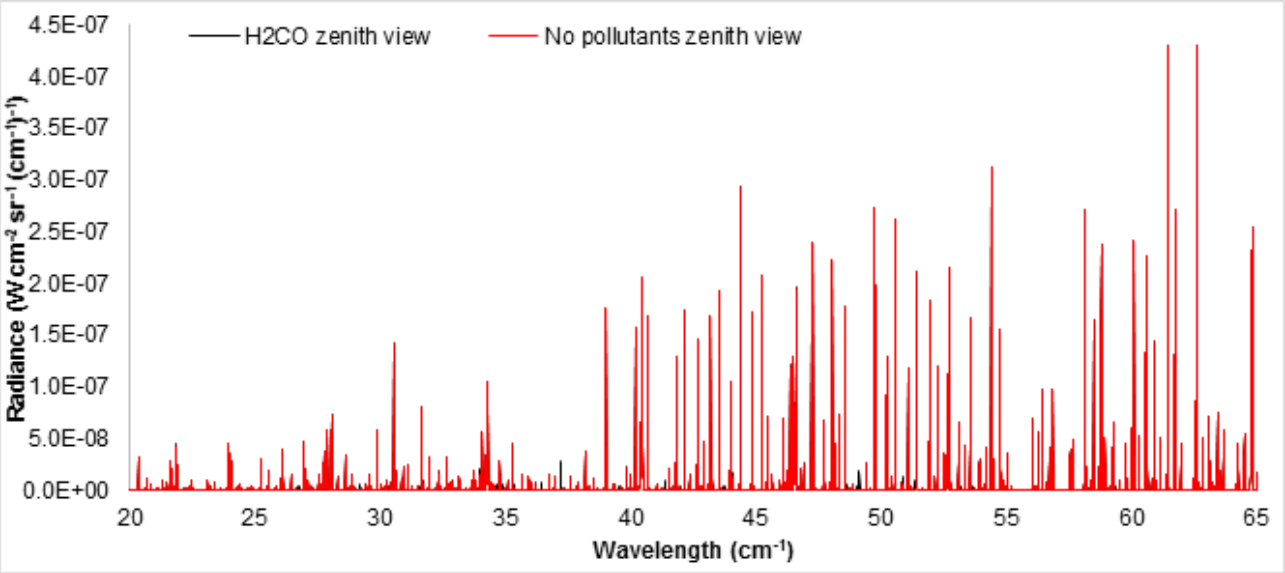

Fig. 3.33: Radiance spectrum with spectral features of the typical concentration of H2CO for a zenith (towards the top of atmosphere) view in a 3 level linearly interpolated atmosphere introduced in par. 2.2

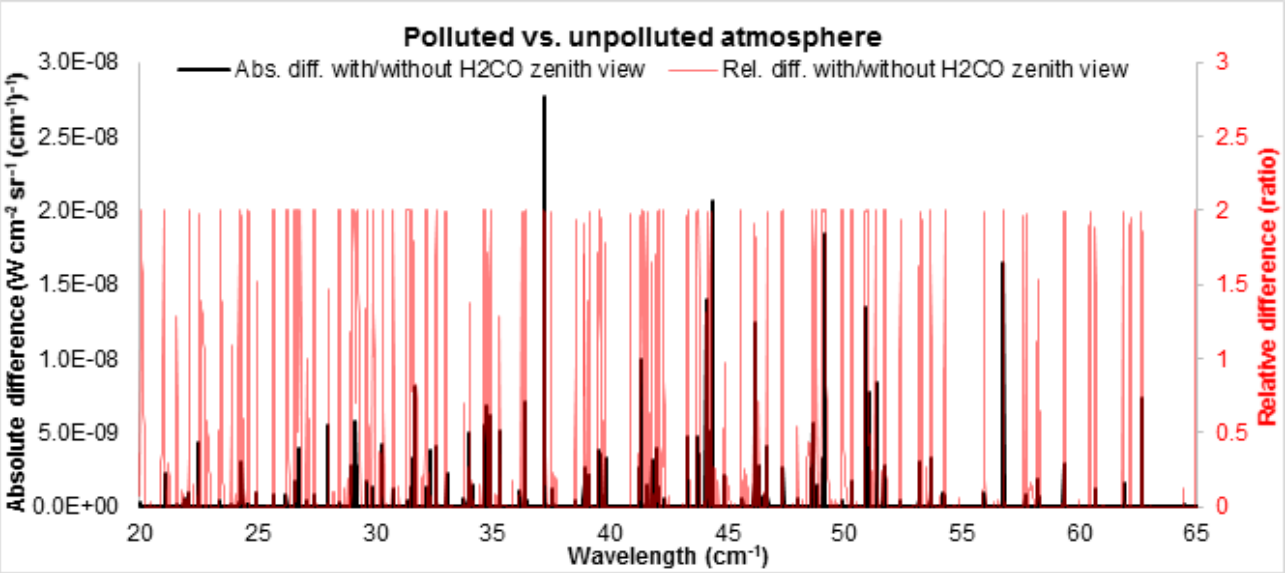

Fig. 3.34: Absolute and relative difference for the radiance spectrum of the atmosphere introduced in par. 2.2 with the typical concentration of H2CO and the corresponding unpolluted atmosphere.

3.3.8 HOCl

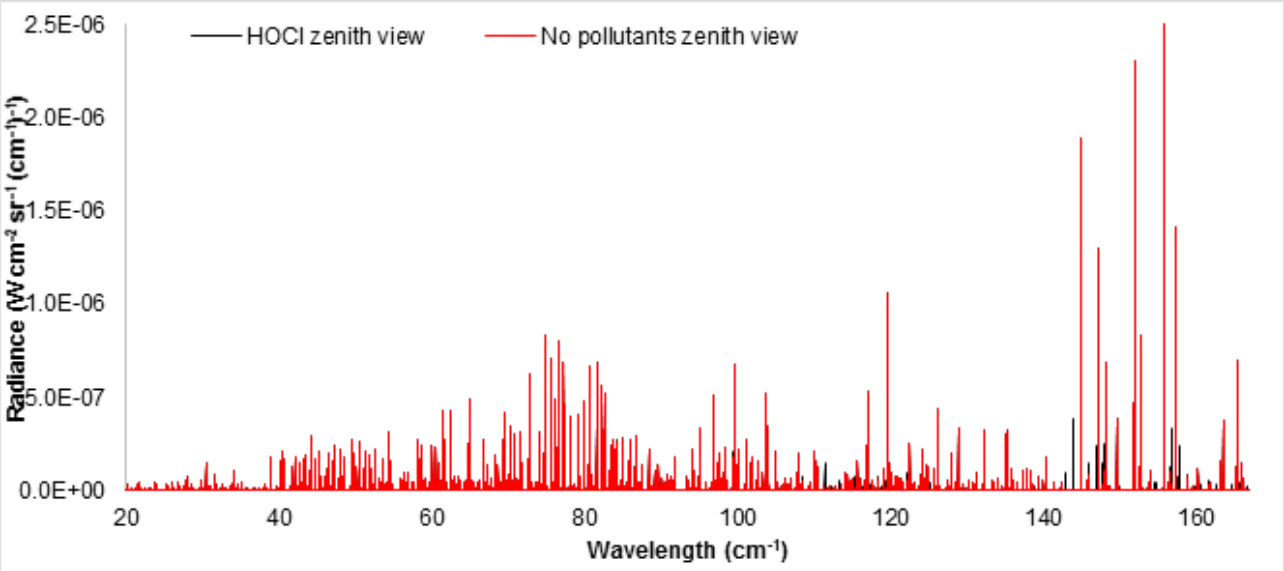

Fig. 3.35: Radiance spectrum with spectral features of the typical concentration of HOCl for a zenith (towards the top of atmosphere) view in a 3 level linearly interpolated atmosphere introduced in par. 2.2

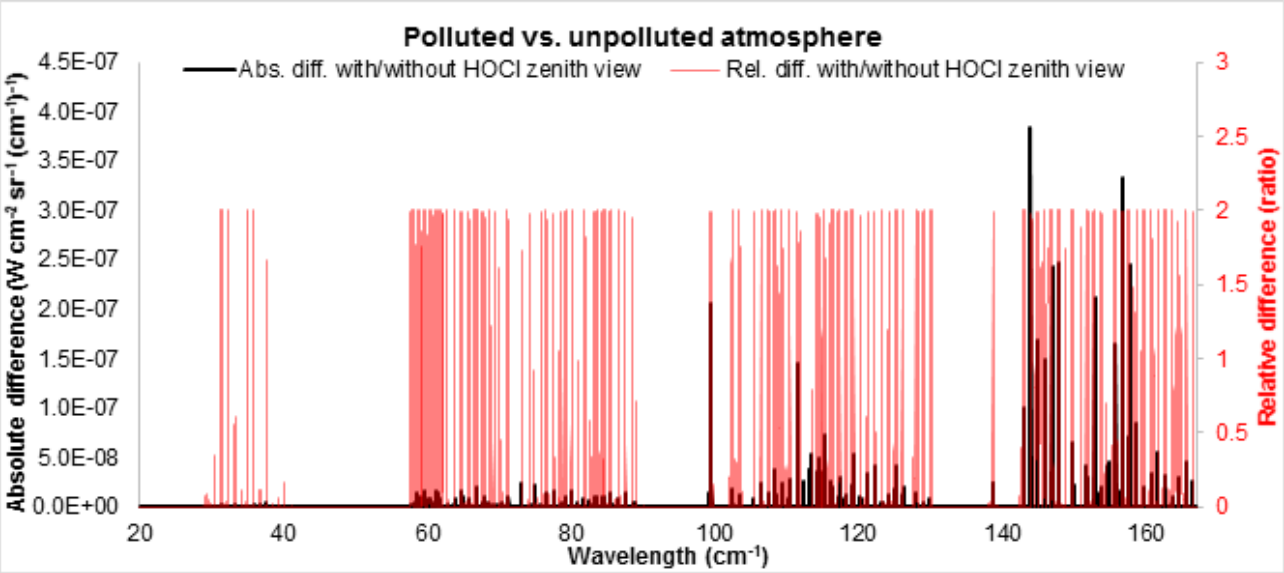

Fig. 3.36: Absolute and relative difference for the radiance spectrum of the atmosphere introduced in par. 2.2 with the typical concentration of HOCl and the corresponding unpolluted atmosphere.

3.3.9 H2S

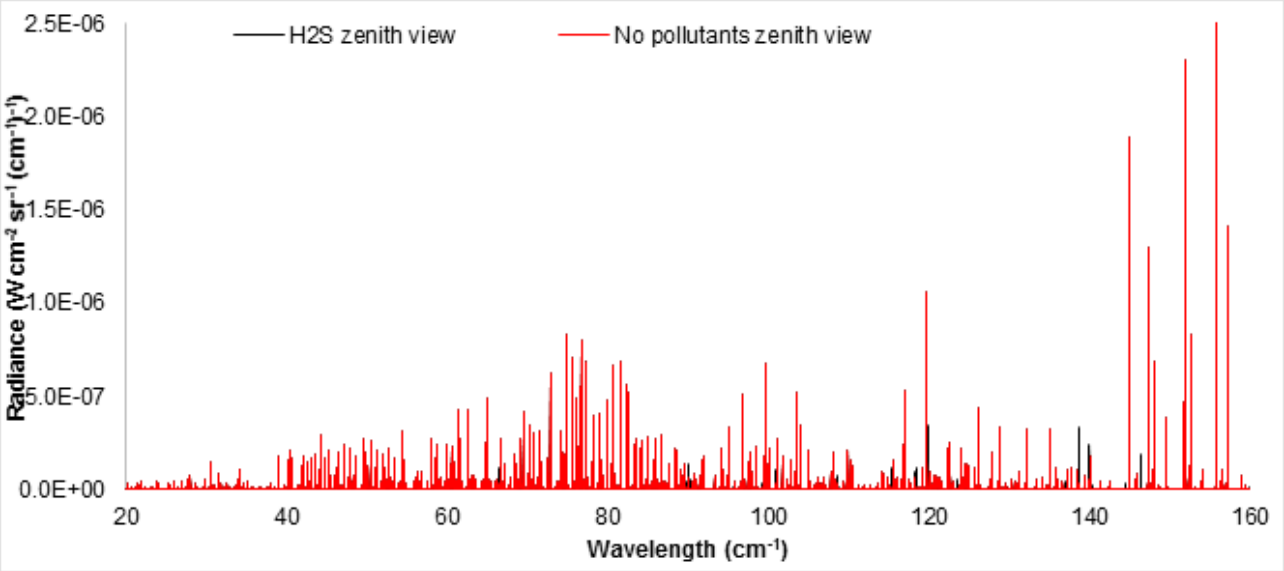

Fig. 3.37: Radiance spectrum with spectral features of the typical concentration of H2S for a zenith (towards the top of atmosphere) view in a 3 level linearly interpolated atmosphere introduced in par. 2.2

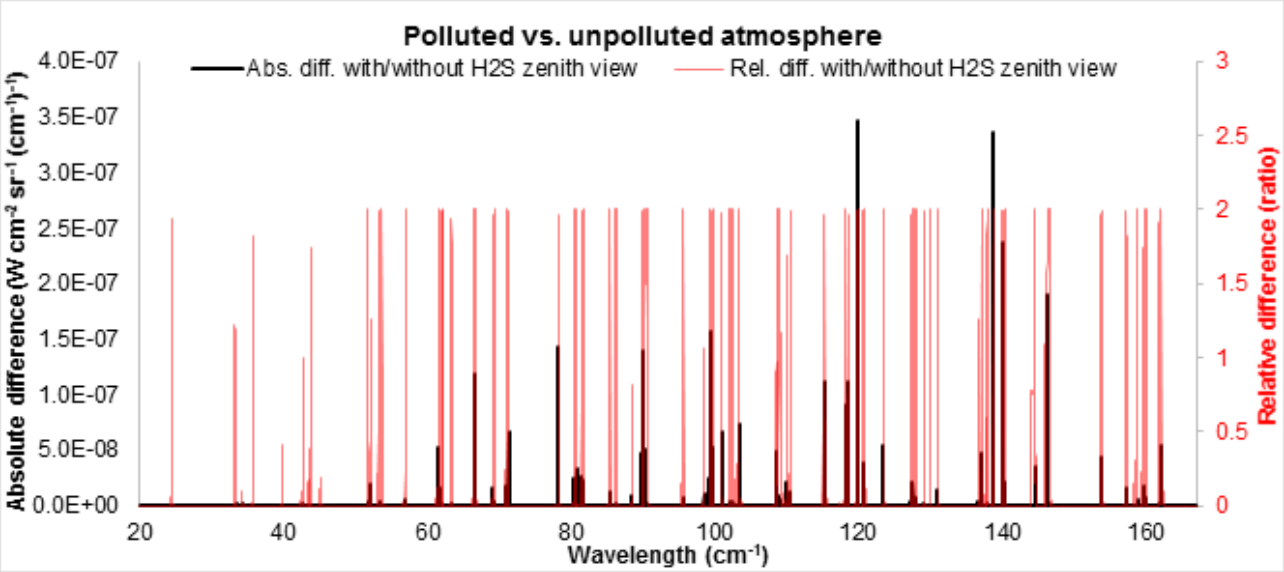

Fig. 3.38: Absolute and relative difference for the radiance spectrum of the atmosphere introduced in par. 2.2 with the typical concentration of H2S and the corresponding unpolluted atmosphere.

3.4 *Equivalent constant layer model*

The terms α_g, α_0, α_1, α_2 introduced in par. 3.2 can be seen as function of the transmittances T_{g0}, T_{01}, T_{12}, $T_{2\infty}$ and emissivity ε_0, ε_1, ε_2 of the layers of an equivalent model with constant (i.e. non-interpolated) absorption coefficients and temperature (Fig. 3.39).

$$\alpha_g = T_{g0}T_{01}T_{12}T_{2\infty}$$
$$\alpha_0 = \varepsilon_0 T_{01}T_{12}T_{2\infty} = (1 - T_{g0})T_{01}T_{12}T_{2\infty}$$
$$\alpha_1 = \varepsilon_1 T_{12}T_{2\infty} = (1 - T_{g0}T_{01})T_{12}T_{2\infty}$$
$$\alpha_2 = \varepsilon_2 T_{2\infty} = (1 - T_{g0}T_{01}T_{12})T_{2\infty}$$

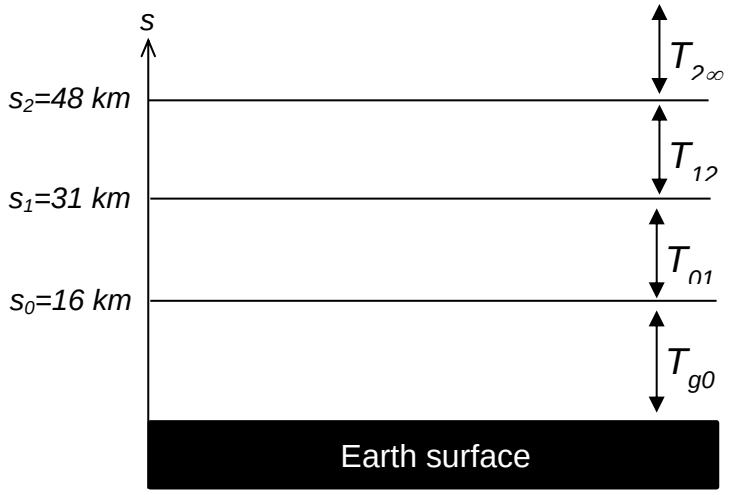

Fig. 3.39: Transmittances of the equivalent constant layers model. Each layer has constant transmittance and temperature. The emissivity of each level can be seen as 1 minus the transmittances of the lower levels.

The inversion of the system brings to the expressions for the equivalent transmittances of the corresponding constant-layer model:

$$T_{g0} = \frac{\alpha_g}{\alpha_g + \alpha_0}$$
$$T_{01} = \frac{\alpha_g + \alpha_0}{\alpha_g + \alpha_1}$$
$$T_{12} = \frac{\alpha_g + \alpha_1}{\alpha_g + \alpha_2}$$
$$T_{2\infty} = \alpha_g + \alpha_2$$

where the terms α_g, α_0, α_1, α_2 have to be calculated considering the absorptions given by all the different species of each level and the right values for Δs_1, Δs_2 (i.e. in case of diagonal crossing of the layer they must be scaled according with the cosine law).

3.5 *Limb view*

Considering the model described in par. 3.1, we modify the equations for taking into account the limb geometry of Fig. 3.40:

$$I(l_n) - I(l_0) = \int_{l_0}^{l_n} \beta_a(l)(B(T(l)) - I(l))dl$$

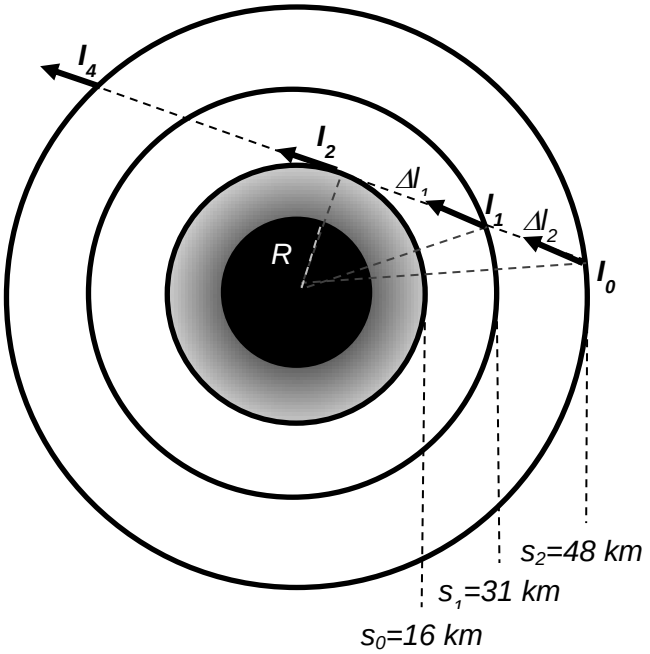

Fig. 3.40: Calculation of dl (a) and geometry of observation for two different limb view geometry in black and red (b).

being l_0,...,l_n the points along the paths l in Fig. 3.40.

Following the linear approximation we have:

$$I_1 = I_0 + \frac{1}{2}\left[\beta_{a_0}(B_0 - I_0) + \beta_{a_1}(B_1 - I_1)\right](l_1 - l_0)$$
$$I_2 = I_1 + \frac{1}{2}\left[\beta_{a_1}(B_1 - I_1) + \beta_{a_2}(B_2 - I_2)\right](l_2 - l_1)$$

For symmetry, it follows also:

$$I_4 = 2I_2$$

We solving the system defining (being R the Earth radius):

$$\Delta l_{01} = l_1 - l_0 = \sqrt{(R + s_1)^2 - (R + s_0)^2}$$
$$\Delta l_{12} = l_2 - l_1 = \sqrt{(R + s_2)^2 - (R + s_0)^2}$$
$$I_0 = 0$$

and we calculate I_1 and I_2 as:

$$I_1 = \frac{\Delta l_{01}\left(\beta_{a_1}B_1 + \beta_{a_0}B_0\right)}{\beta_{a_1}\Delta l_{01} + 2}$$
$$I_2 = \frac{\left(\beta_{a_1}\Delta l_{01} + 2\right)\beta_{a_2}\Delta l_{12}B_2 + 2(\Delta l_{12} + \Delta l_{01})\beta_{a_1}B_1 + \left(2 - \beta_{a_1}\Delta l_{12}\right)\beta_{a_0}\Delta l_{01}B_0}{\left(\beta_{a_1}\Delta l_{01} + 2\right)\beta_{a_2}\Delta l_{12} + 2\beta_{a_1}\Delta l_{01} + 4}$$
$$I_4 = 2\frac{\left(\beta_{a_1}\Delta l_{01} + 2\right)\beta_{a_2}\Delta l_{12}B_2 + 2(\Delta l_{12} + \Delta l_{01})\beta_{a_1}B_1 + \left(2 - \beta_{a_1}\Delta l_{12}\right)\beta_{a_0}\Delta l_{01}B_0}{\left(\beta_{a_1}\Delta l_{01} + 2\right)\beta_{a_2}\Delta l_{12} + 2\beta_{a_1}\Delta l_{01} + 4}$$

or, as for the nadir view case without ground contribution:

$$I_4 = 2(\alpha_2 B_2 + \alpha_1 B_1 + \alpha_0 B_0)$$

with:

$$\alpha_0 = \frac{(2 - \beta_{a_1}\Delta l_{12})\beta_{a_0}\Delta l_{01}}{(\beta_{a_1}\Delta l_{01} + 2)\beta_{a_2}\Delta l_{12} + 2\beta_{a_1}\Delta l_{01} + 4}$$

$$\alpha_1 = \frac{2(\Delta s_2 + \Delta s_1)\beta_{a_1}}{(\beta_{a_1}\Delta l_{01} + 2)\beta_{a_2}\Delta l_{12} + 2\beta_{a_1}\Delta l_{01} + 4}$$

$$\alpha_2 = \frac{(\beta_{a_1}\Delta l_{01} + 2)\beta_{a_2}\Delta l_{12}}{(\beta_{a_1}\Delta l_{01} + 2)\beta_{a_2}\Delta l_{12} + 2\beta_{a_1}\Delta l_{01} + 4}$$

3.5.1 NO2

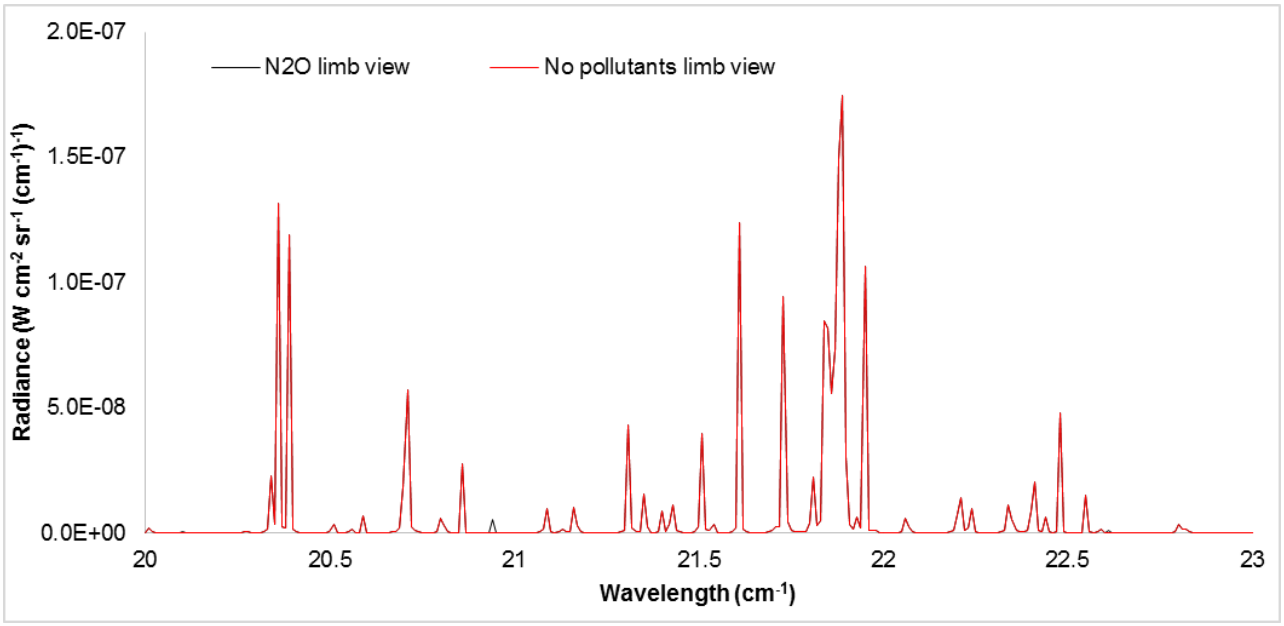

Fig. 3.41: Radiance spectrum with spectral features of the typical concentration of N2O for limb view in a 3 level linearly interpolated atmosphere introduced in par. 2.2.

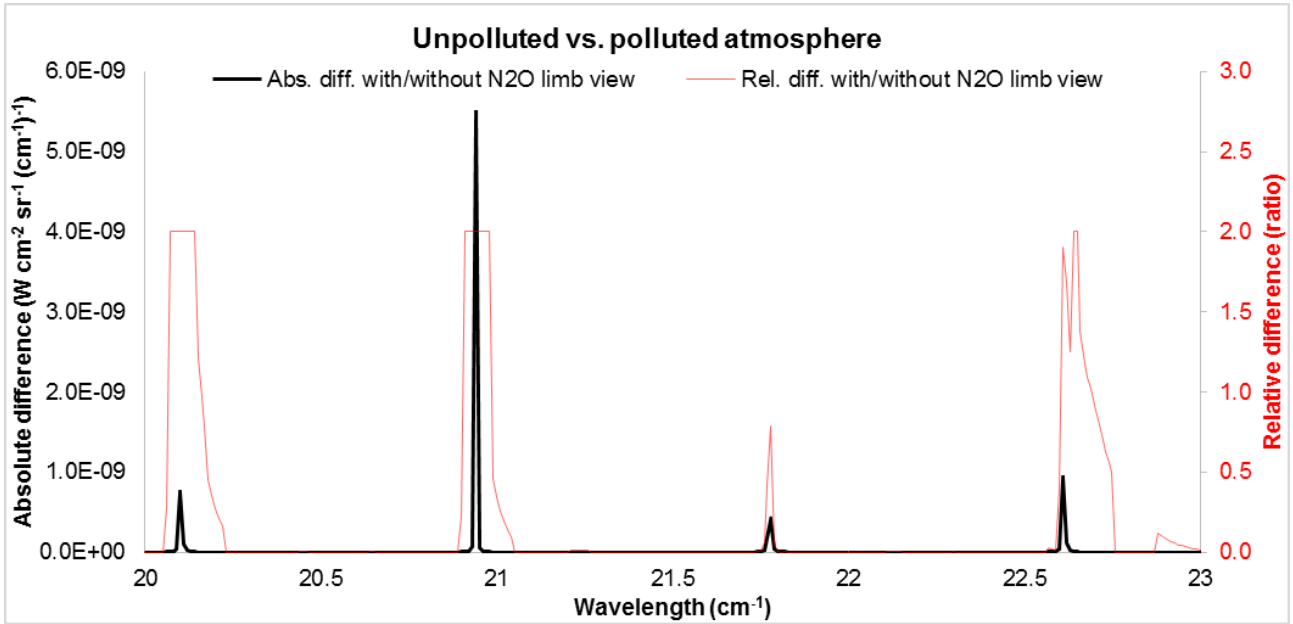

Fig. 3.42: Absolute and relative difference for the radiance spectrum of the unpolluted atmosphere introduced in par. 2.2 and the same atmosphere with the typical concentration of N2O.

3.5.2 CO

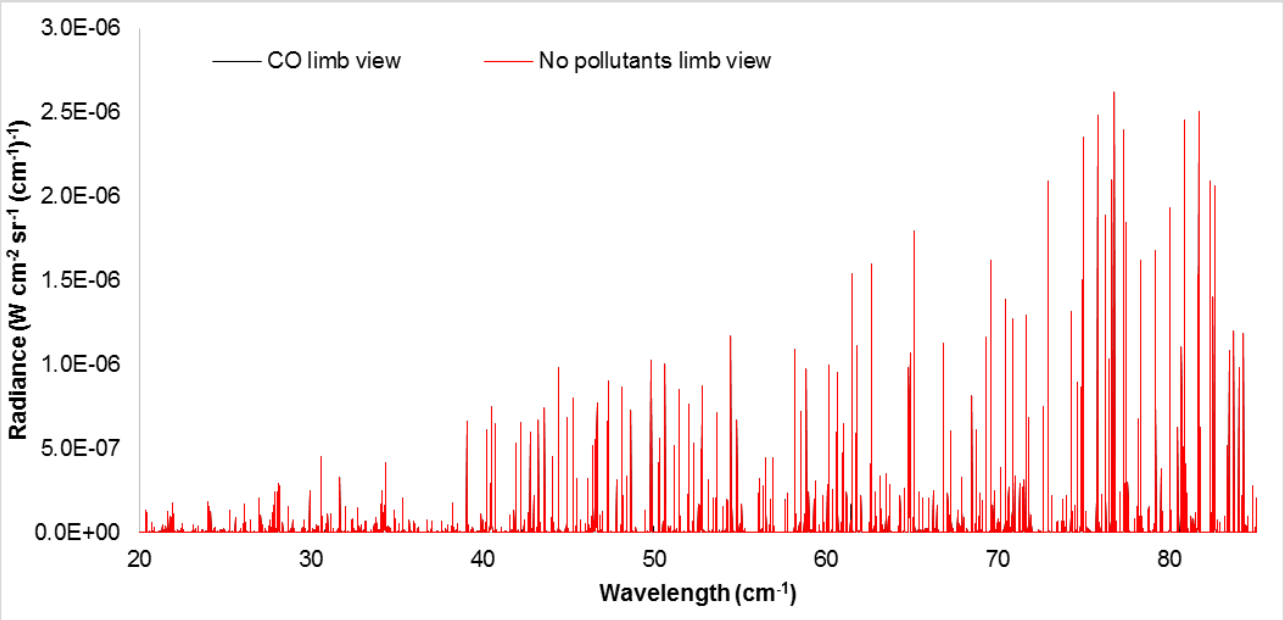

Fig. 3.43: Radiance spectrum with spectral features of the typical concentration of CO for limb view in a 3 level linearly interpolated atmosphere introduced in par. 2.2

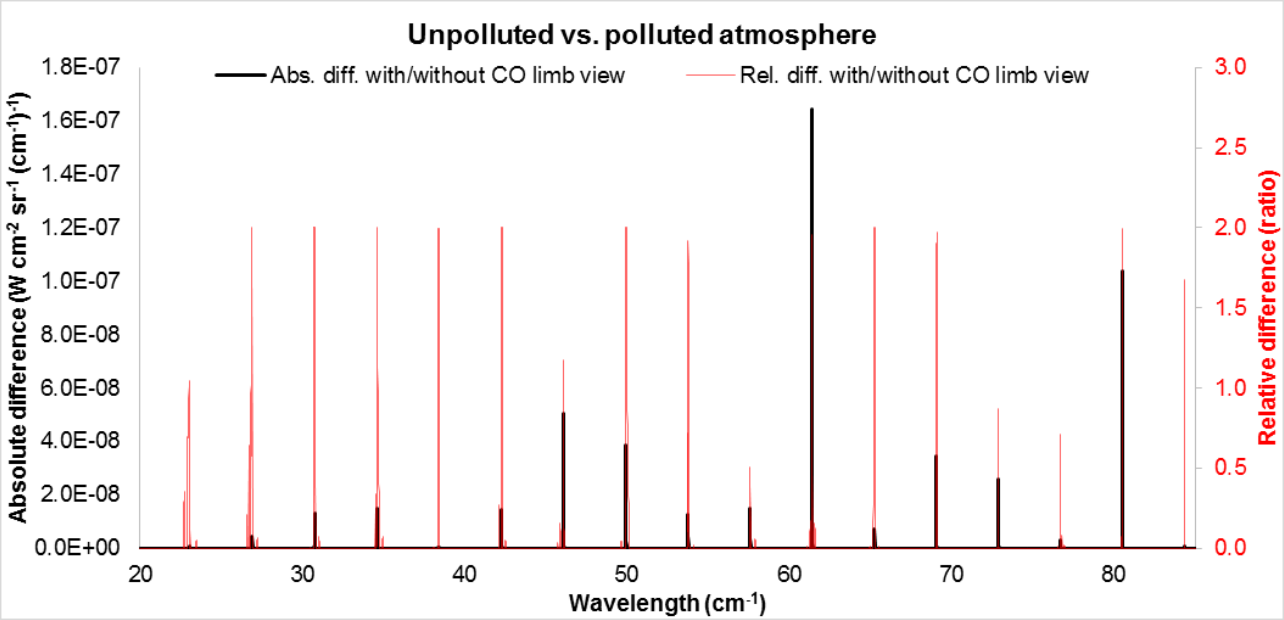

Fig. 3.44: Absolute and relative difference for the radiance spectrum of the unpolluted atmosphere introduced in par. 2.2 and the same atmosphere with the typical concentration of CO.

3.5.3 SO2

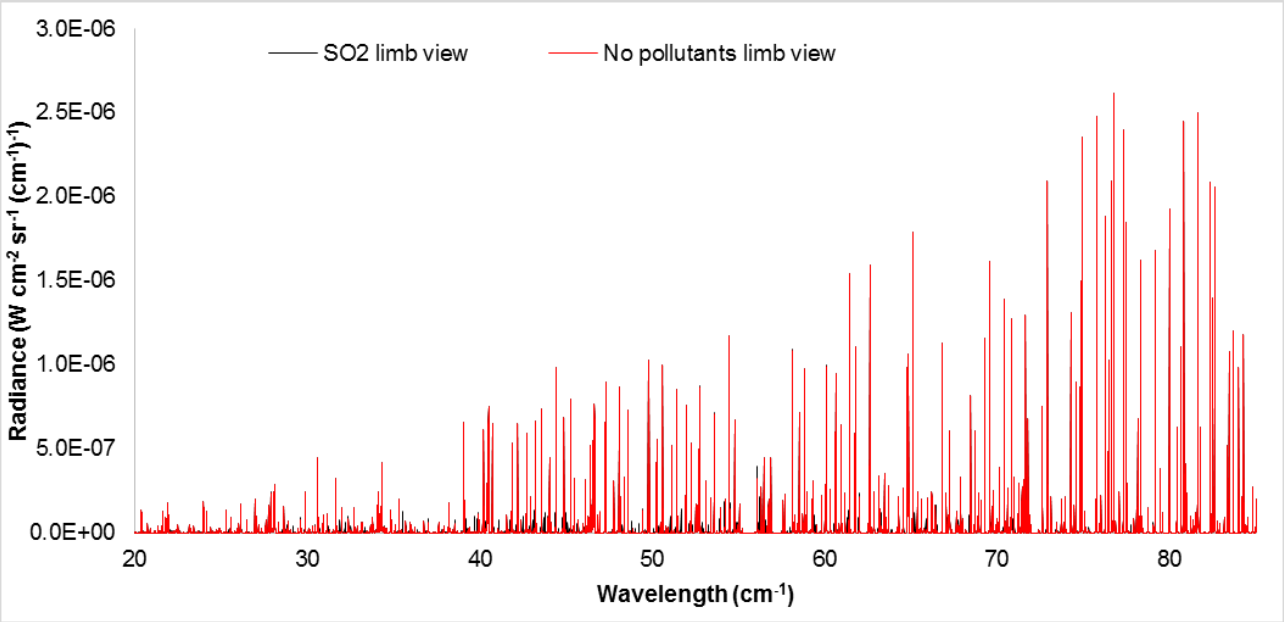

Fig. 3.45: Radiance spectrum with spectral features of the typical concentration of SO2 for limb view in a 3 level linearly interpolated atmosphere introduced in par. 2.2

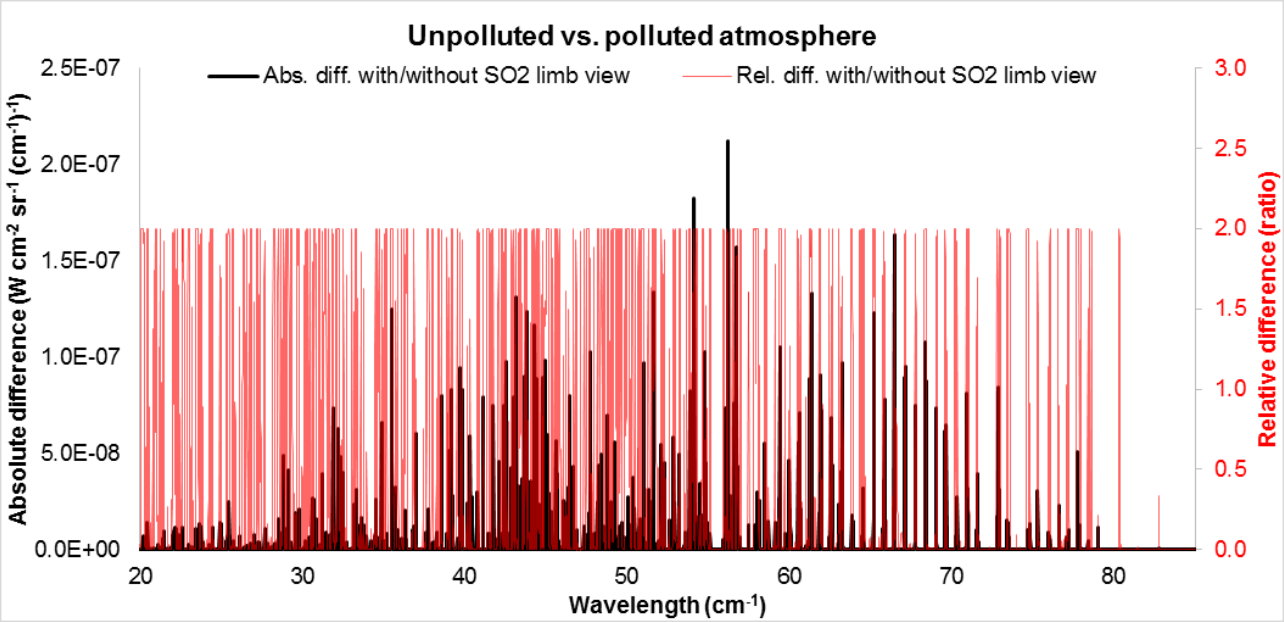

Fig. 3.46: Absolute and relative difference for the radiance spectrum of the unpolluted atmosphere introduced in par. 2.2 and the same atmosphere with the typical concentration of SO2.

3.5.4 NH3

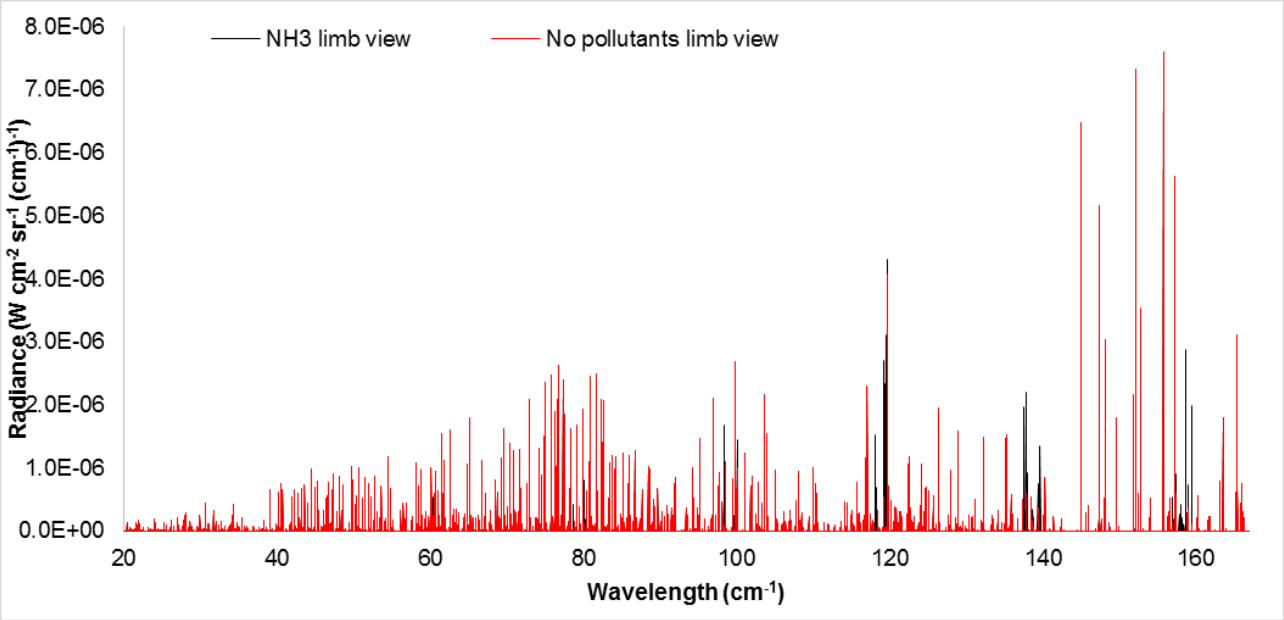

Fig. 3.47: Radiance spectrum with spectral features of the typical concentration of NH3 for limb view in a 3 level linearly interpolated atmosphere introduced in par. 2.2

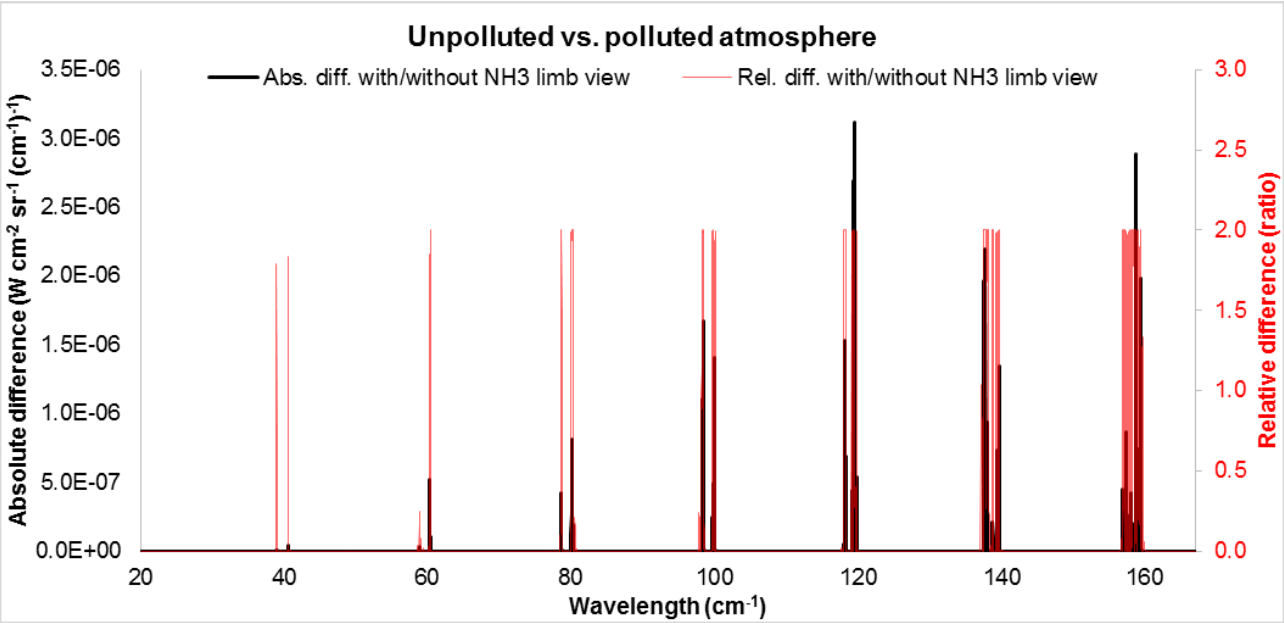

Fig. 3.48: Absolute and relative difference for the radiance spectrum of the unpolluted atmosphere introduced in par. 2.2 and the same atmosphere with the typical concentration of NH3.

3.5.5 OH

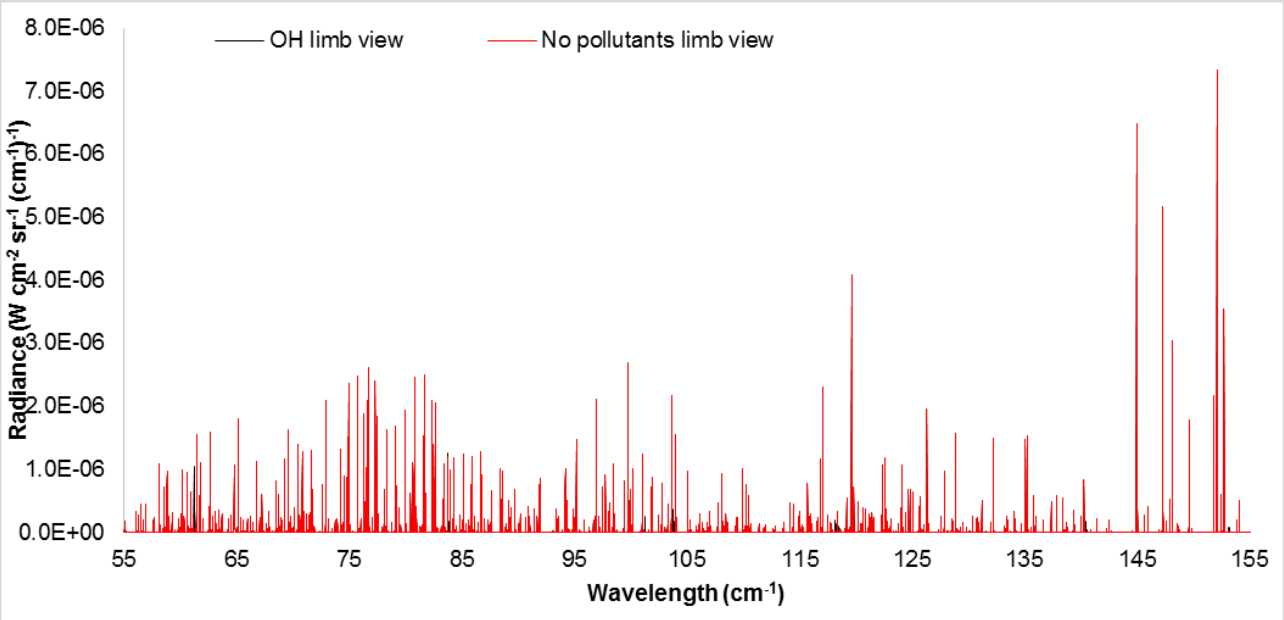

Fig. 3.49: Radiance spectrum with spectral features of the typical concentration of OH for limb view in a 3 level linearly interpolated atmosphere introduced in par. 2.2

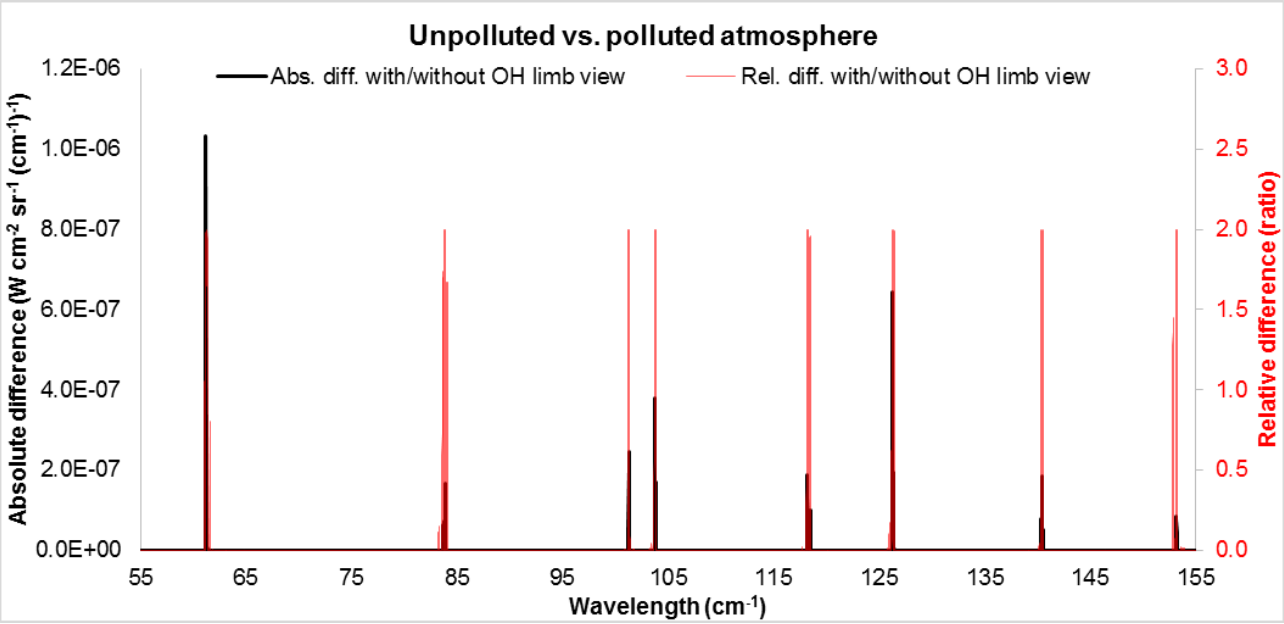

Fig. 3.50: Absolute and relative difference for the radiance spectrum of the unpolluted atmosphere introduced in par. 2.2 and the same atmosphere with the typical concentration of OH.

3.5.6 HCl

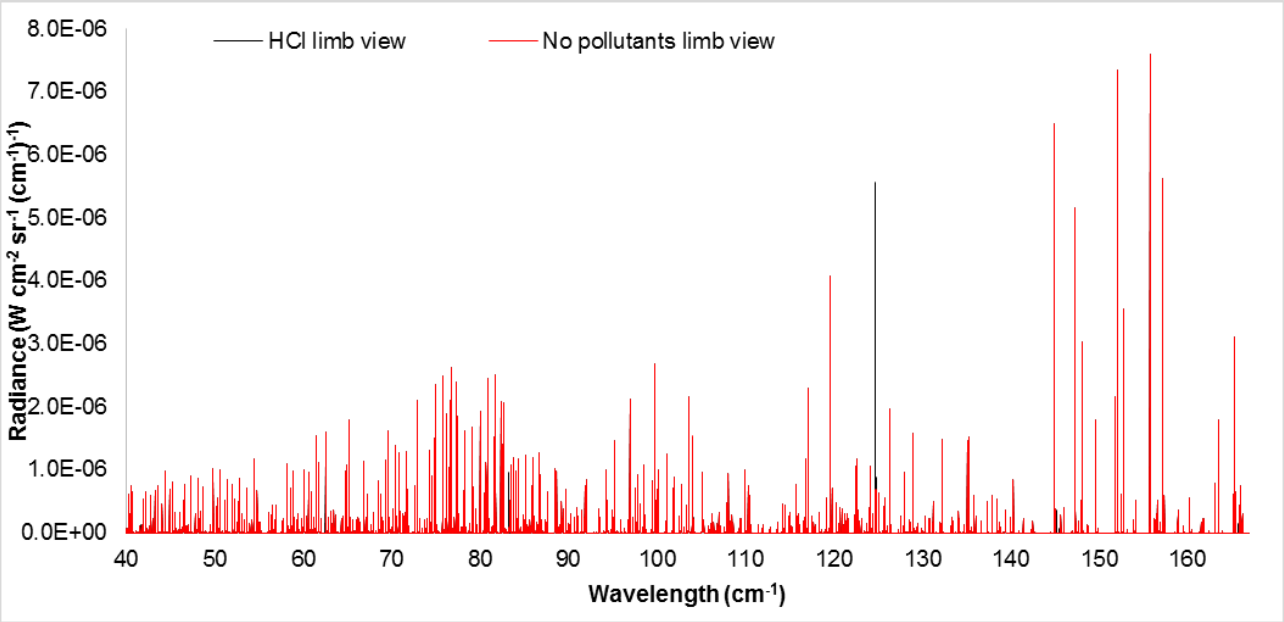

Fig. 3.51: Radiance spectrum with spectral features of the typical concentration of HCl for limb view in a 3 level linearly interpolated atmosphere introduced in par. 2.2

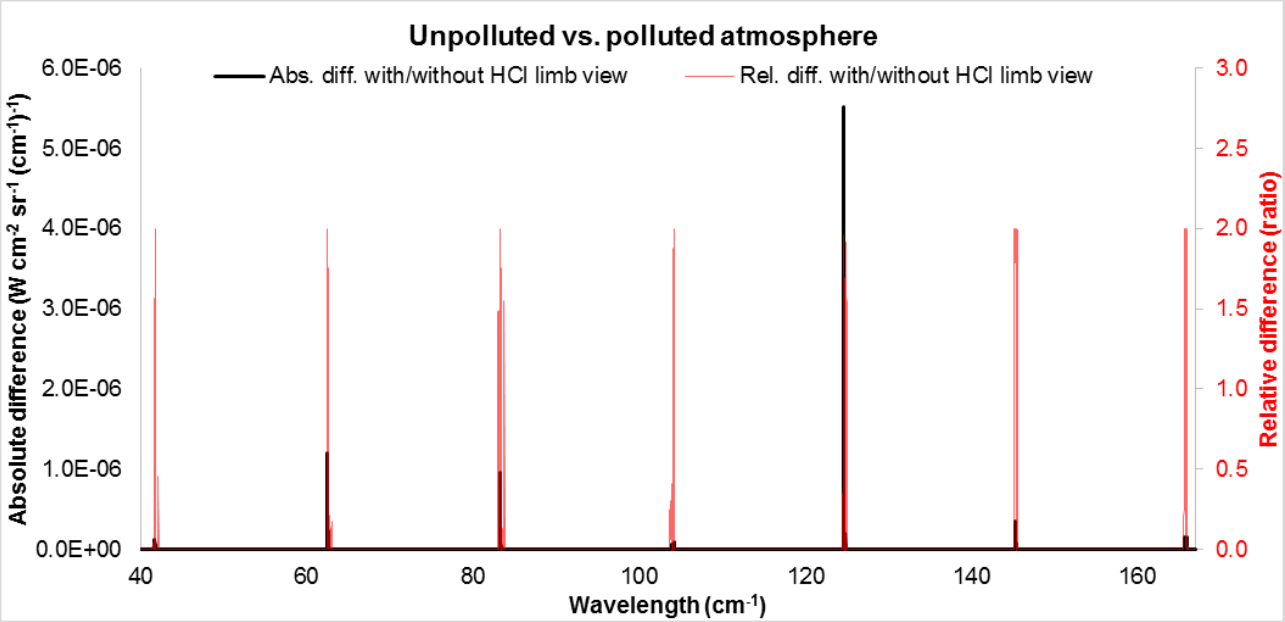

Fig. 3.52: Absolute and relative difference for the radiance spectrum of the unpolluted atmosphere introduced in par. 2.2 and the same atmosphere with the typical concentration of HCl.

3.5.7 H2CO

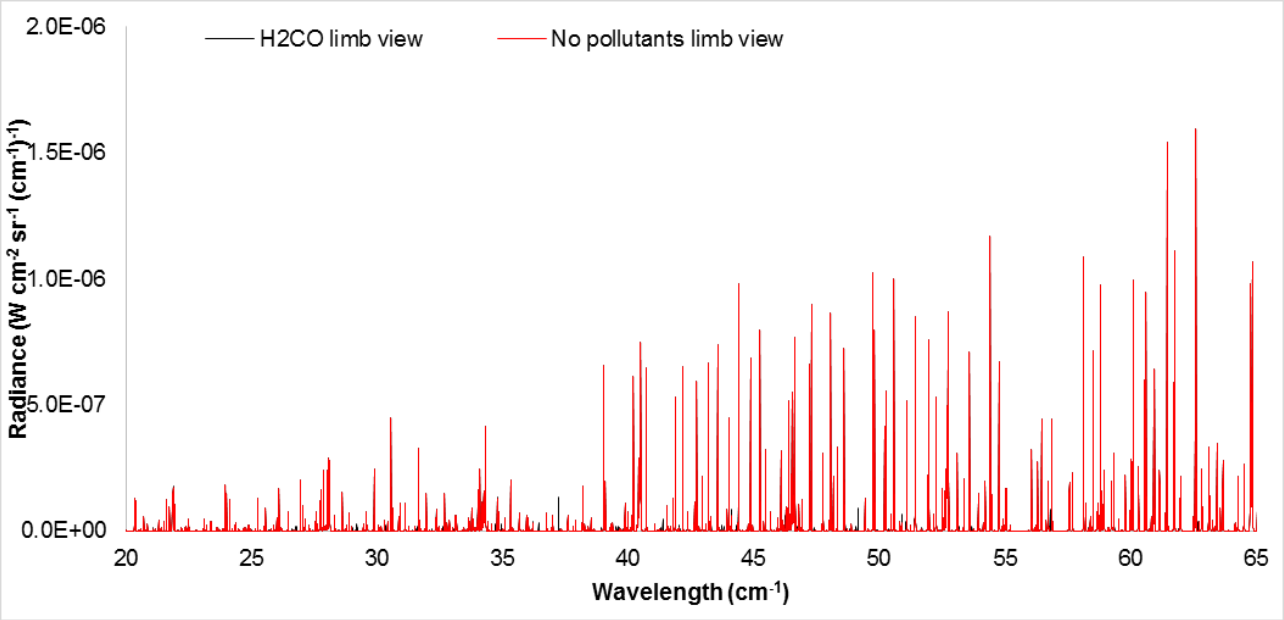

Fig. 3.53: Radiance spectrum with spectral features of the typical concentration of H2CO for limb view in a 3 level linearly interpolated atmosphere introduced in par. 2.2

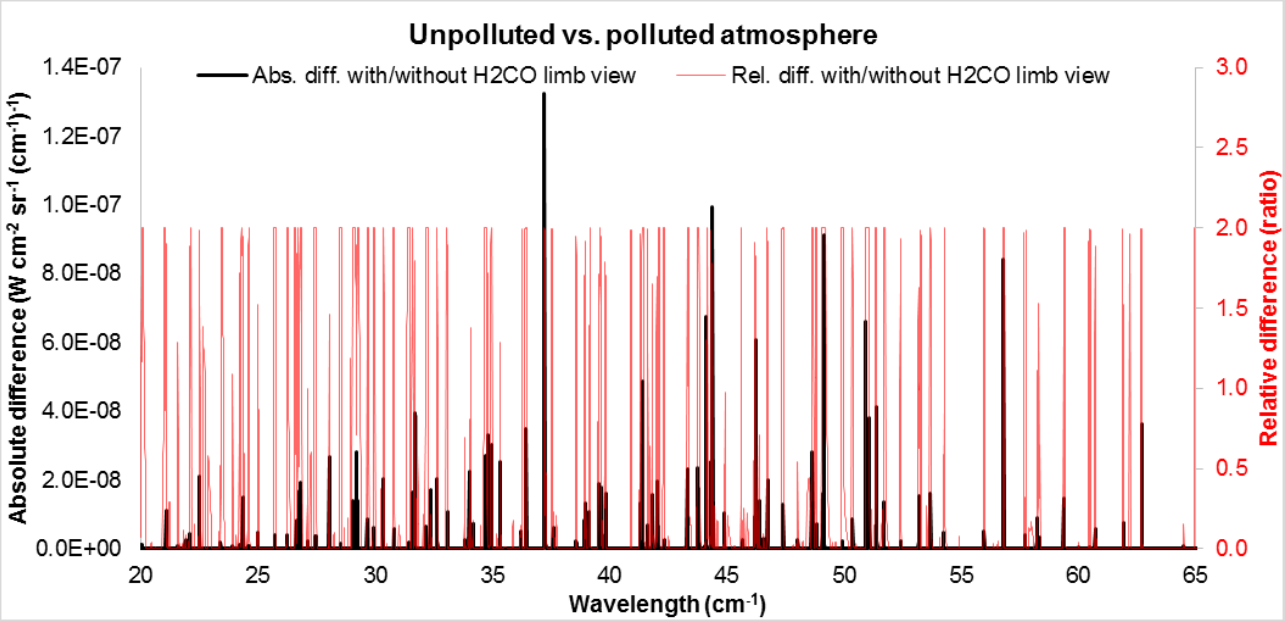

Fig. 3.54: Absolute and relative difference for the radiance spectrum of the unpolluted atmosphere introduced in par. 2.2 and the same atmosphere with the typical concentration of H2CO.

3.5.8 HOCl

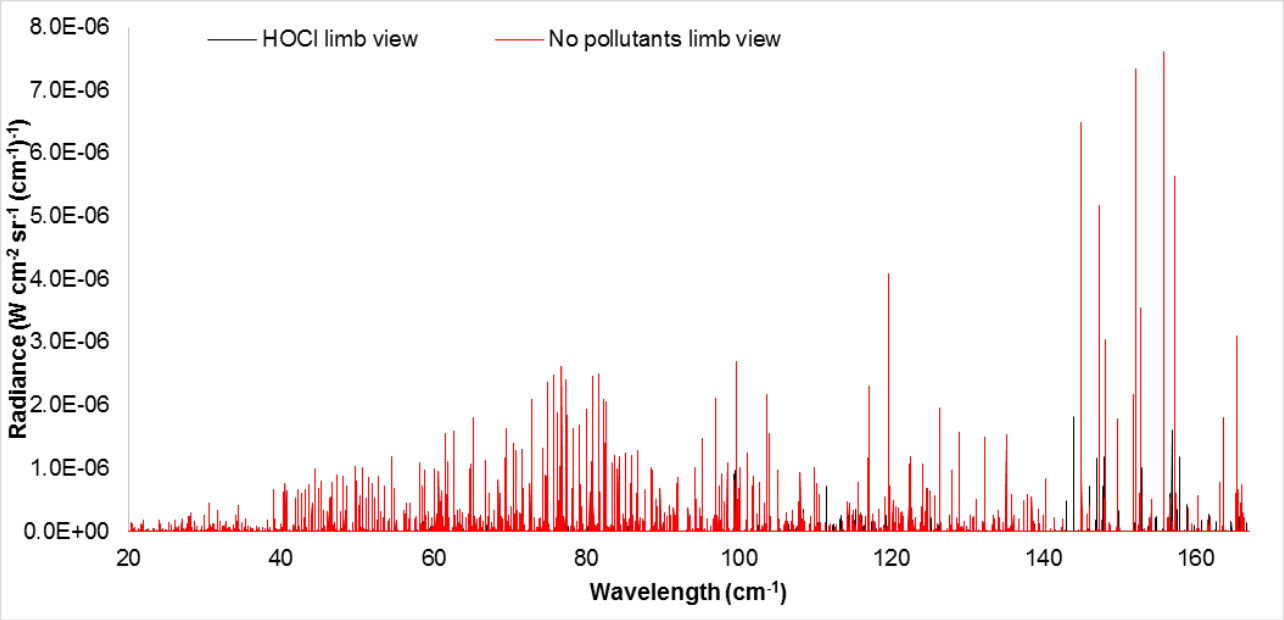

Fig. 3.55: Radiance spectrum with spectral features of the typical concentration of HOCl for limb view in a 3 level linearly interpolated atmosphere introduced in par. 2.2

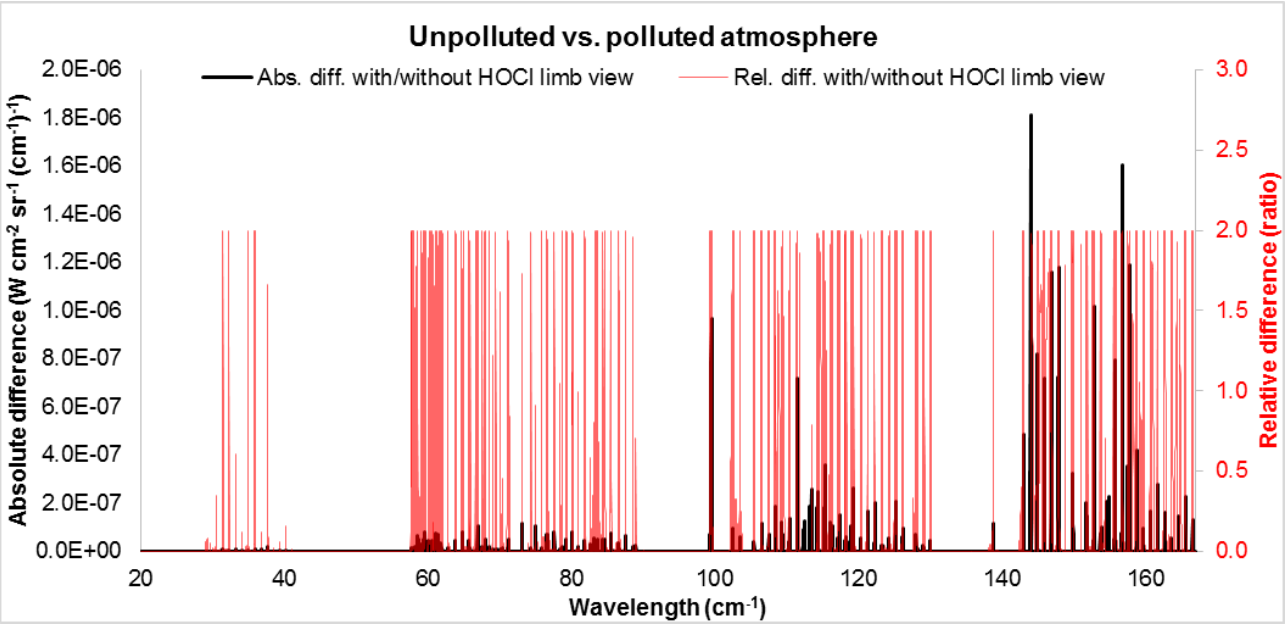

Fig. 3.56: Absolute and relative difference for the radiance spectrum of the unpolluted atmosphere introduced in par. 2.2 and the same atmosphere with the typical concentration of HOCl.

3.5.9 H2S

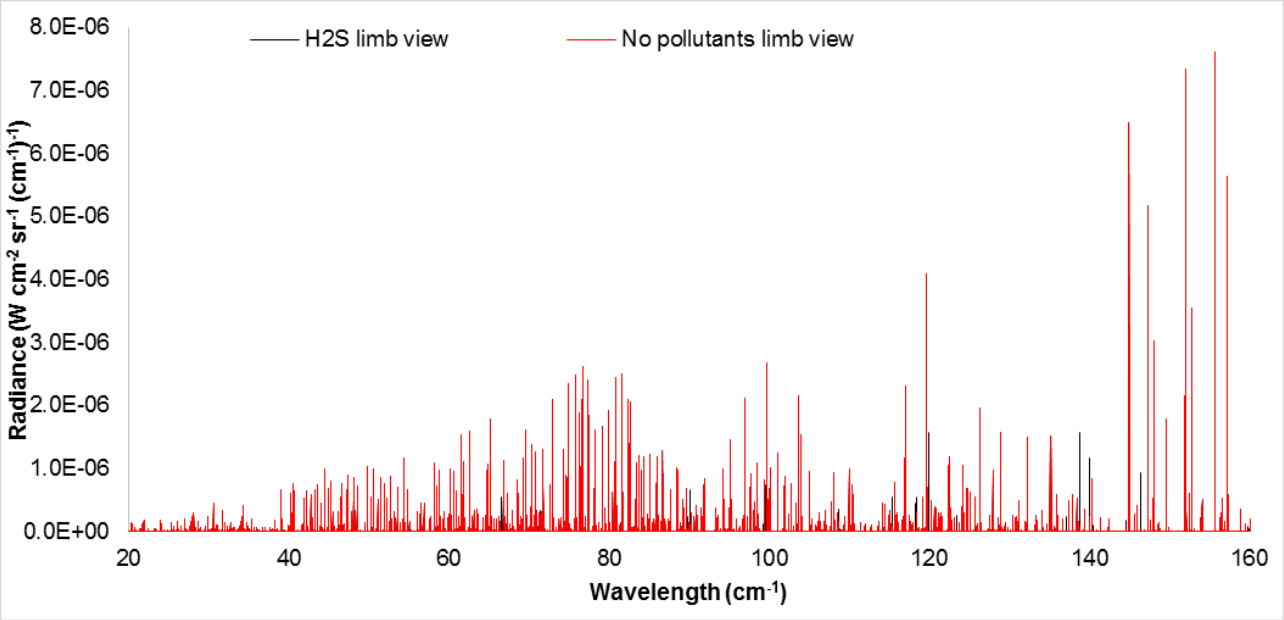

Fig. 3.57: Radiance spectrum with spectral features of the typical concentration of H2S for limb view in a 3 level linearly interpolated atmosphere introduced in par. 2.2

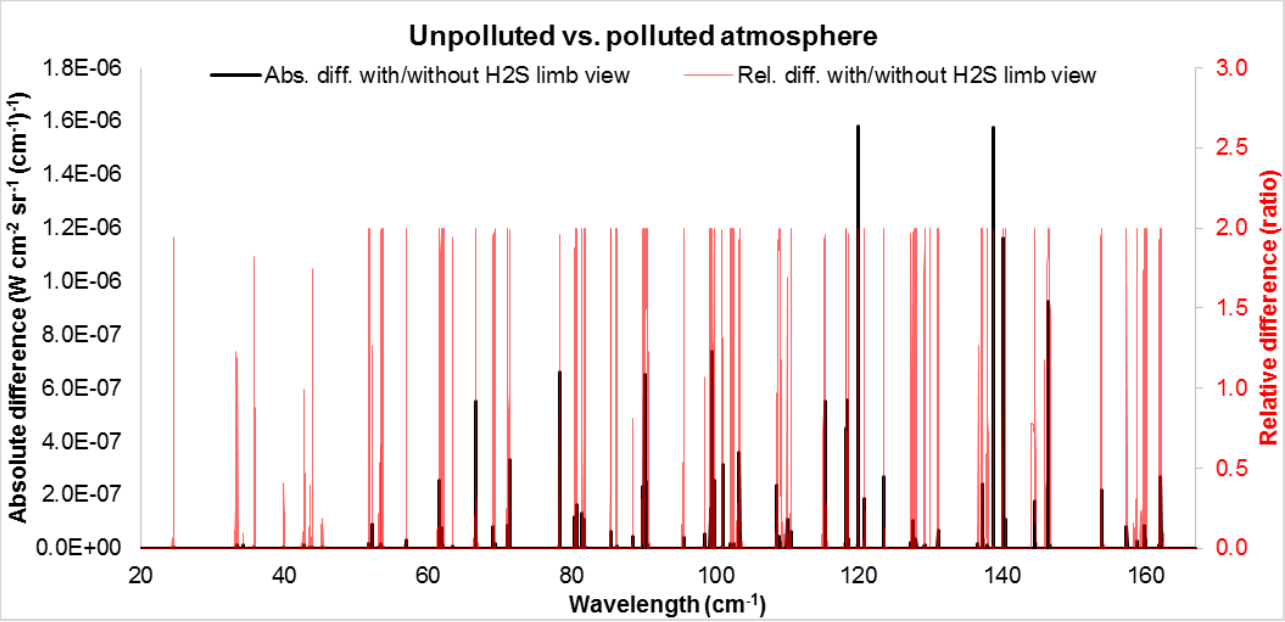

Fig. 3.58: Absolute and relative difference for the radiance spectrum of the unpolluted atmosphere introduced in par. 2.2 and the same atmosphere with the typical concentration of H2S.

4 Conclusions

This report shows the main characteristics of atmospheric absorbers in the terahertz spectral region, being the interval of interest in the framework of DIAST project. The simulated atmospheres presented in this document have being considered for the designs of different kind of spectroradiometers. The estimate of the instrumental characteristic SNR has been performed for different line of sight in typical working scenarios as a function of the integration time and bandwidth.